Impacts of Sea Level Rise on Future Storm-induced Coastal Inundations over Massachusetts Coast

Changsheng Chen[1], Zhaolin Lin[1], Robert C. Beardsley[2], Tom Shyka[3], Yu Zhang[4], Qichun Xu[1], Jianhua Qi[1], Huichan Lin[1], and Danya Xu[5]

[1]University of Massachusetts-Dartmouth, New Bedford, MA 02744
[2]Woods Hole Oceanographic Institution, Woods Hole, MA 02543
[3]Northeastern Regional Association of Coastal Ocean Observing Systems (NERACOOS), Portsmouth, NH 03801
[4]College of Marine Sciences, Shanghai Ocean University, Shanghai, 201306, P. R. China
[5]Southern Marine Science and Engineering Guangdong Laboratory, Zhuhai, 519082, China

Corresponding author: Changsheng Chen < c1chen@umassd.edu>

Contributing authors:
Robert C Beardsley <rbeardsley@whoi.edu>
Zhaolin Lin<zlin@umassd.edu>
Tom Shyka<tom@neracoos.org>
Huichan Lin <hlin@umassd.edu>
Jianhua Qi <jqi@umassd.edu>
Qichun Xu < qxu@umassd.edu>
Yu Zhang< yuzhang@shou.edu.cn>

Key Points:

1. Sea level rise will aggravate the storm-induced coastal inundation.

2. Sea level rise will strengthen surface waves and thus increase flood risk from wave runup-induced overtopping.

3. Responses of surge and wave runup to sea level rise are fully nonlinear and required to be investigated with wave-current interactions.

This paper is published on Natural Hazard, http://doi.org/10.1007/c11069-020-04467-x.

Abstract

Hurricanes (tropical cyclones) and nor'easters (extratropical cyclones) are two major storm systems for flood risk over the Massachusetts coast. Severe coastal inundation usually happens when wind-induced waves and storm surges coincide with high tides. A Northeast Coastal Ocean Forecast System (NECOFS) was established and placed into the 24/7 forecast operations starting in 2007. Using a well-validated "end to end" FVCOM inundation model of NECOFS, we examined the impact of climate change-induced sea-level rise (SLR) on the future extratropical storms-induced coastal inundation over the Massachusetts coast. The assessment was done by making the model experiments to project the storm-induced inundation over the coastal areas of Scituate and Boston Harbors with different SLR scenarios under a hundred-year storm condition. The results suggest that with sustained SLR, the northeastern US coast will be vulnerable more severely to wave runup-induced splashing/overtopping than wind-induced storm surges. This finding is consistent with the change in the intensity of storm-generated surface waves in the last decade. The model also suggests that the responses of surge and surface waves to SLR are fully nonlinear. The assessment of the impacts of SLR on the future storm-induced coastal inundation should be investigated with a model including wave-current interactions.

1. Introduction

The Massachusetts (Mass) coast (Fig.1) was often attacked by nor'easters (extratropical storms) and hurricanes (tropical storms). At high tides, combined wind-sea waves and wind-induced surges caused severe flooding in the regions susceptible to storms (*Beardsley et al*., 2013; *Chen et al*., 2013). In the last four decades, hundreds of storms struck the Mass coast, most of them produced severe coastal inundation with infrastructure damage and economic loss (Bernier and Thompson, 2006; McCown, 2008; *Freedman*, 2013).

Over the Mass coast, the coastal inundation is caused by storm surges and wave runup-induced splashing/overtopping (A. Mignone, personnel communication). The former is mainly caused by storm-induced rising of the sea level, while the latter is a complex runup and breaking process of nonlinear transformation waves that spread and fraction on rigid structures. Over the coast vulnerable to storm surges, steep or vertical seawalls are commonly built along the coastline to protect the coast against flooding. It works well to protect from surge-induced coastal flooding but not for wave runup-induced water splashing/overtopping (*Allsop et al*., 2005). The wave breaking, fragmentation, sprays, and flooding are characterized by the kinematics of fluid flows with intricate free surface patterns, which can be simulated by introducing an infrastructure-resolving transient numerical hydrodynamic models for wave breaking, runup, and overtopping on rigid structures (*Gómez-Gesteira et al*., 2012a-b, *Brizzolara et al*., 2008 and 2011). However, most of these models take a significant computational time for a few day simulations and are not realistic to be used for the forecast of coastal inundation at present.

The mean sea level has significantly risen over the U.S. northeastern coast in the last decades, with a trend following the IPCC (the Intergovernmental Panel on Climate Change) projection (*IPCC*, 2007, *Rahmstorf*, 2010, *Pritchard et al*., 2012; *Hellmer et al*., 2012). We collected the elevation data at ten tidal gauges along the New England coast and used a linear regression method to project SLR (Fig.2). Ten stations from north to south were Halifax in Canada; Eastport, ME; Portland, ME; Boston, MA; Woods Hole, MA; Nantucket, MA; Newport, RI; New London, CT; Montauk, NY; New York, NY. The results show that Montauk experienced the fastest SLR, while the slowest was at Portland. At Portland, an SLR of ~0.18 cm per year is still higher than an average yearly SLR of 0.17 cm worldwide, implying that SLR will have a more significant impact on storm-induced flooding in the New England region. A recent assessment of the effect of SLR on predicted changes in the intensity and paths of hurricanes in the North Atlantic shows that New York City will experience significantly more severe storm surges in the future (*Lin et al*., 2012).

There is a critical need to quantitatively assess the impact of SLR on the Mass coastal region. Since the coastal inundation along the Mass coast is a complex process manifested through the nonlinear interaction of winds, currents, and waves over topography (*Chen et al*., 2013), it is imperative to establish a coastal inundation model system for this region. The desired outcomes of such a system should include 1) warning of coastal flooding on an event timescale to facilitate evacuation and other emergency measures to protect human life and property in the coastal zone, and 2) accurate estimation of the statistics of coastal inundation to enable rationale planning regarding sustainable land-use practices in the coastal area. The functional requirements for this system are a) accurate, real-time forecasting of water level at high spatial resolution (order 10 m or less) in the coastal zone, including estimates of uncertainty, and b) accurate estimates of the statistics of water level and inundation areas (one year, ten years, hundred years, etc.) in response to SLR.

We developed a Northeast Coastal Ocean Forecast System (NECOFS) (http://134.88. 228.119:8080/fvcomwms/) and placed it into research-oriented forecast operations in late 2007. NECOFS includes four "end-to-end" sub-domain inundation models for Scituate Harbor, Boston Harbors, MA, Hampton River, NH, and Saco Bay, ME. These inundation models were validated through comparisons with observed vital variables, including total water level, tidal elevation, surge level, wave height, flooding area, etc. (e.g., *Chen et al.,* 2013, *Beardsley et al.,* 2013). To predict the wave runup-induced water splashing or overtopping over seawalls, we also implemented the *Allsop et al.* (2005) sloping seawall overtopping forecast model into NECOFS.

Using a well-validated “end-to-end” coastal inundation forecast model system under the framework of NECOFS, we examined the impact of SLR on extratropical storm-induced coastal inundation in the Mass coastal region. This study aims to provide the state with a quantitative assessment that could help either in decision-making policy or developing strategies for future protection on coastal infrastructure as well as coastal zone management in sustainable land-use practices, coastal conservation, and habitat restoration.

The impacts of SLR on storm-induced coastal inundation are intensively examined in the tropical region, especially in the Gulf of Mexico (e.g., *Bilskie et al.,* 2014, 2016; 2019; *Taylor et al., 2015*; *Passeri et al*. 2015a, 2015b, 2016). A typical low-elevation landscape characterizes the coast of the Gulf of Mexico is characterized by a typical low-elevation, which is at a high risk to SLR. *Bilskie et al.* (2014) used the Advanced Circulation (ADCIRC) model to assess the responses of hurricane-induced storm surge to SLR with consideration of change of land surface elevation in the future. They found that responses are fully nonlinear, especially to landscape changes. A comprehensive review of the dynamic effects of SLR on the Gulf of Mexico was given by *Passeri et al.* (2015a). Similar to the Gulf of Mexico, many coastal areas around Mass contain similar landscapes, mudflat, tidal creeks, and vegetation, which are all vulnerable to SLR. This study focused on the storm-induced flooding over harbors with seawalls, with no efforts to examine the change of landscapes in the region.

This paper summarizes the numerical experiments' findings from assessing the SLR's impact on coastal inundations in Boston and Scituate Harbors of Mass Bay, MA. The remaining sections are organized as follows. Section 2 describes NECOFS inundation models and designs of numerical experiments. Section 3 presents the results of model validation through the comparison with observational data. Section 4 highlights the change of coastal inundation for different scenarios of SLR under a hundred-year storm condition. Section 5 discusses the dynamics driving these changes, and conclusions are summarized in Section 6.

2. The Inundation Model and Designs of Numerical Experiments

2.1 The Inundation Model

NECOFS is an integrated atmosphere, surface waves, and ocean forecast model system designed for the U.S. northeast coastal region. The upgraded ocean domain of NECOFS covers the continental shelf, coastal bays, inlets, and estuaries from Cape Hatteras to the eastern end of the Scotian Shelf. The subdomain inundation forecast/hindcast models of NECOFS were developed using fully three-dimensional (3D) current-wave coupled modules of the Finite Volume Community Ocean Model (FVCOM) (*Chen et al.*, 2003; 2006a, 2013a). FVCOM is the sea ice, currents, waves, and sediment coupled model system with options to run under either hydrostatic or non-hydrostatic assumption. It utilizes the second-order approximate finite-volume discrete algorithm with an integral form of governing equations over momentum and tracer control volumes in the terrain-following generalized vertical coordinate system with either Cartesian coordinates (*Chen et al*., 2003) or spherical coordinates (*Chen et al*., 2006b, 2013a). FVCOM is numerically solved with options of either a mode-split solver in which external and internal modes are advanced in tandem at two different time steps (*Chen et al*., 2003) or a semi-implicit solver with a single time step (*Chen et al*., 2011; *Lai et al.*, 2010a-b).

The wave model in FVCOM is SWAVE, an unstructured-grid version of the simulating waves nearshore model (SWAN) solved by a second-order approximate, either semi-implicit or mode-split, finite-volume discrete method (*Qi et al*., 2009). SWAVE is coupled with FVCOM through the surface, and radiation stresses in the momentum equations and the bottom stress with the inclusion of wave-current interactions in the bottom boundary layer (BBL) (*Wu et al.,* 2010). The BBL code used in coupling was converted from the code developed by *Warner et al*. (2008) under an unstructured grid framework of FVCOM.

In the vertical, mixing in FVCOM is parameterized with options of either Mellor-Yamada level 2.5 turbulence submodel as a default setup (*Mellor and Yamada*, 1982) or the General Turbulence Model (GOTM) (*Burchard,* 2002). In the horizontal, the diffusion was parametrized using the Smagorinsky turbulent parameterization method (*Smagorinsky*, 1963). The detail of governing equations and discrete algorithms of FVCOM can be found in FVCOM User Manual (*Chen et al*. 2013a).

The inundation model was configured with the high-resolution (1-m×1-m) LIDAR bathymetry data, including the land and water in the Mass coastal zone. The coastal inundation was simulated using a 3-D flooding/drying treatment method in FVCOM (*Chen et al.*, 2003, 2006a,b, 2008). A quadratic formula was used for bottom friction parameterization. When the dry cell turned to wet, the bottom friction used in the water is applied. Over the land turning to wet, the MY2.5-produced vertical diffusion is vertically averaged and then applied to resolve the wet-dry areas. The wet-dry point treatment method was first validated by comparing the water level and flooded area with remote sense-derived hypsometric data and current measurement along tidal creeks in the Okatee/Colleton River in South Carolina. The results were summarized in the FVCOM user manual with the detail given in an unpublished manuscript (*Chen, C., H. Huang, H. Lin, J. Blanton, C. Li, F. Andrade, A wet/dry point treatment method of FVCOM, part II: application to the Okatee/Colleton River in South Carolina*). This method was also validated for wetland-estuarine-shelf water exchange in the Satilla River, GA (*Chen et al.*, 2008), the Plum Island Sound-Merrimack River complex, MA (*Zhao et al*., 2010), Scituate Harbor, MA (Beardsley et al. 2013, *Chen et al*., 2013) and tidal simulation in the Gulf of Maine (GoM) and Mass Bay (*Chen et al*., 2011).

2.2. Design of numerical experiments

We selected Scituate and Boston Harbors as two study sites. Both of these two sites are extremely susceptible to extratropical and tropical storm-induced flooding (Fig.1). Scituate Harbor is a coastal lagoon connected to a wide area of wetland and saltmarsh (Fig. 1). The mean water depth varies from ~15 m over the shelf to ~5-6 m in the harbor's deeper area. Boston Harbor is a large harbor adjacent to Boston's city on the west and open to the outer Mass Bay through the exit with Winthrop and Nantasket Peninsulas on the north and south, respectively (Fig.1). This harbor is characterized by complex irregular coastal geometry with considerable numbers of islands. The mean water depth varies from ~35 m in the outer harbor to ~2-4 m in the inner harbor.

We configured the inundation models for Scituate and Boston Harbors using an unstructured triangular grid nesting with the NECOFS regional FVCOM domain (Fig. 3). The horizontal resolution varied from ~ 400-500 m in the outer harbor to ~10 m in the inner harbor and over the land near the coast (Fig.3). In the vertical, a total of 10 uniform σ-layers were specified, with a vertical resolution varying from 1.5 m over the shelf to 0.1 m or less along the coast where the water depth was 1.0 m or less. The models were driven by the MM5-assimilated meteorological forcing at the surface. MM5 is the 5th-generation NCAR/PSU non-hydrostatic, terrain-following, sigma-coordinate mesoscale weather model developed jointly by the National Center for Atmospheric Research (NCAR) and Pennsylvania State University (PSU) [*Dudhia and Bresch*, 2002, *Dudhia et al.,* 2003]. The NECOFs regional FVCOM hydrodynamical and wave models provided the inundation model's boundary conditions, including the real-time sea-level elevation (with tidal and subtidal components), significant wave heights/peak periods, temperature/salinity at boundary nodes, and 3-D velocities in the centroid of boundary triangles.

The USGS-streamflow records were used to determine the freshwater discharge at each river. Initial fields of elevation, temperature/salinity, currents, significant wave heights/peak periods were specified using the NECOFS regional ocean/wave models. The SWAVE's parameters were the same as those used in *Beardsley et al*. (2013) and *Chen et al*. (2013).

We conducted the storm return probability analysis using the 39-year (1978-2016) wind records on Buoy#44013 in Mass. A storm was defined when the local wind exceeded 0.2 Pa (25 mph) and lasted at least 6 hours (*Butman et al.,* 2008). In the past 39 years, there were a total of 364 storms that struck Mass Bay. For inundation applications, the storm return period was defined based on return periods of storm-induced water elevation at a tidal gauge in Boston Harbor over 1922-2016. An online NOAA-recommended standard program was adopted for the probability analysis of the storm return year with the water elevation records (Fig.4). In the last 95 years, only the February 1978 nor'easter produced the water elevation of > 3.0 m. It was accounted for a 1% probability of the return water level, by which we defined it as a 100-year storm. Based on the same definition, the January 1987 nor'easter was a 50-year storm, whereas December 1959, February 1972, January 1979, October 1991, December 1992, May 2005, April 2007, and January 2014 nor'easters were 10-year storms. In this study, the assessment is focused on the 100-year storm of the February 1978 Blizzard. According to the water level record, the 1991 Hurricane Bob was a ten-year storm for Buzzard Bay but not for Boston Harbor/Mass Bay. We simulated this storm with an aim at comparing hurricane and nor'easter-induced coastal inundations.

In February 1978, the northerly or northeasterly (blowing from the north) wind prevailed over the entire New England Shelf. The outbreak of a nor'easter appeared on February 5 and lasted for about four days. The northeasterly wind appeared at 03:00:00 GMT on February 7, with a maximum of > 20 m/s throughout the day (*Altimari*, 1998). On that day, the gusts were up to ~ 50 m/s (*Earls and Dukakis*, 2008). We used MM5 to rebuild the wind and air pressure fields for this storm. The resulting sea level pressure and wind vectors at the 10-m height were shown in Fig.5. Although there was no data to validate the accuracy of the model-predicted wind field, the temporal variation, and intensity of the simulated wind were consistent with the storm scenarios described by *Altimari* (1998) and *Earls and Dukakis* (2008).

Hurricane Bob moved into the U.S. northeastern coast and traversed over southern New England and the GoM on August 19-20, 1991. It originally appeared as a tropical storm in the Atlantic Ocean on August 16 and strengthened as it moved northwestward and became "Hurricane Bob" on August 17. Hurricane Bob first brushed the North Carolina shelf on August 18-19, during which it reached H3 with maximum sustained winds of 51.4 m/s. Shortly after that, on August 19, Hurricane Bob weakened to H2 and made landfall near Newport, Rhode Island (*Sun et al*., 2013). As it re-entered Mass Bay from the land, it had already weakened to become a tropical storm, with maximum winds of ~15 m/s (Fig. 5). Sun *et al*. (2013) rebuilt the fields of winds and barometric air pressure using a combined MM5 and hurricane model. The results were validated through the comparison with observational data. The calibrated wind and air pressure data were used in this study.

The inundation models for Boston and Scituate Harbors were validated through comparisons with observed total, tidal, and surge water levels at tidal gauges as well as the sea level pressure, winds, and waves at Buoy#44013. The potential impact of SLR on future flooding was examined and estimated by running the model with different SLR scenarios. The inundation maps for the cases with SLR of 0.0-7.0 ft were created. To quantify the roles of the current-wave interaction process in simulating the surface elevation and waves, we also conducted the numerical experiments for the cases with and without the inclusion of wave-current coupling.

3. Simulation Results

3.1. The 1978 nor'easter and 1991 Hurricane Bob simulations

The inundation model for Scituate Harbor was validated for nor'easters sweeping the Mass coast on May 24-27, 2005 and April 17-20, 2007 (*Chen et al*., 2013) as well as December 27, 2010 (*Beardsley et al*. 2013). With an improved boundary tidal forcing, the error of maximum water level reduced to 1.3 cm, with a difference of < 1.0 cm at the peak (*Beardsley et* al. 2013). The FVCOM-based inundation model was a three-dimensional model capable of resolving the vertical flow structure and coastal upwelling. The simulations for the 2005 and 2007's nor'easters were done as the U.S. national inundation model testbed experiment by comparing other two-dimensional inundation models, including ADCIRC (*Chen et al*., 2013).

The inundation model for Boston Harbor was validated for water elevation at the tidal gauge in the harbor. The model-predicted and observed tidal elevations matched well, with uncertainties of 3.0 cm in amplitude and 5^{o} in phase. The model captured the observed maximum surge at high tide, even though the root-mean-square errors (RMSE) were 29.0 and 19.0 cm for the 1978 nor'easter and 1991 Hurricane Bob, respectively (Fig.6). For the 1978 February nor'easter, the model over- and under-predicted the lowest and highest total water levels around the maximum wind period, respectively. It suggested that the local mean sea level changed during the storm, which was not captured by the model. For the 1991 Hurricane Bob, the model also under-estimated the highest total water level, even though the surge was over-estimated.

The changes of local mean sea level during these two storms were caused by a regional adjustment of the sea level to the wind-induced water transport. Therefore, the under-prediction of the total sea level was likely due to the errors in wind predictions, especially in wind direction. The MM5 was replaced by WRF (Weather Research and Forecast) in 2007 with improvements for storm simulation (*Chen et al*., 2013, *Beardsley et al*., 2013). For the 1991 Hurricane Bob simulation, MM5 reasonably re-produced the sea level pressure and winds, with RMSEs of 2.2 hPa in air pressure, 1.5 m/s in wind speed, and 45.3^{o} in wind direction. The wind speed error resulted in an over-prediction of surface waves, with RMSEs of 0.5 m in significant wave height and 2.1 sec. in peak period at Buoy#44013 (Fig.7).

During the February 1978 nor'easter, the maximum water level in Boston Harbor occurred around 16:00:00 GMT on February 7. The sea level rose rapidly over the eastern and western Boston coast, with a high water level of > 2.0 m (Fig.8: upper-left panel). The sustained northeasterly wind pushed the water towards the beach and into Boston Harbor during the flood-tidal period (Fig. 9: left panel). The interaction of wind-driven and tidal currents and surface waves produced a complex geometrically-related circulation inside the harbor. The highest water level occurred in the regions where the flow moved towards the coast. In many inner harbor areas, the maximum total water level was close to or exceeded 3.0 m at high tide. The surface waves were dominated by wind-sea waves, with the maximum significant wave height of > 8.0 m in the outer harbor (Fig.8: upper-right panel). The significant wave height damped significantly when the waves propagated into the port. At Buoy#44013, it dropped to ~3.0 m.

The 1991 Hurricane Bob traversed through Mass Bay during August 19-20, with maximum winds and minimum sea-level pressure occurring around 20:00:00 GMT on August 19. Differing from nor'easters, the wind direction of Hurricane Bob varied spatiotemporally. The maximum surge elevation happened during the transition period from ebb to flood tide. The highest total water elevation occurred in the outer harbor at 20:00:00 GMT on August 19 after the wind peak (Fig.8: lower-left panel). At that time, the significant wave height was about ~2.0 m (Fig. 8: lower-right panel). At the tidal transition, the southern harbor area was dominated by an offshore flow, even though a strong wind-induced inflow was found in that region one hour before the transition (Fig. 9: right panel).

When Hurricane Bob swept Mass Bay, Scituate Harbor was predominated by an offshore wind so that no significant flooding happened in the harbor. For the February 1978 nor'easter, the highest total water elevation occurred at 16:00:00 GMT on February 7. The distributions of water elevations, currents, and significant wave heights were very similar to those described in *Chen et al*. (2013) for May 24-27, 2005 and April 17-20, 2007 nor'easters and in *Beardsley et al*. (2013) for December 27, 2010, nor'easter (Fig. 10).

3.2. Impacts of SLR on future storm-induced coastal inundations

Taking the February 1978 nor'easter as a hundred-year storm, we ran the inundation models for Boston and Scituate Harbors by taking the projected SLRs of 1.0, 2.0, 3.0, 5.0, and 7.0 ft into account. The changes in surface elevations, surface waves, and inundation area with SLR are described here.

Surface elevations and waves. Under the same wind condition, the climate-induced SLR could significantly increase the intensity of surface waves and cause a higher water elevation around the coast. The increases in the water elevation and significant wave heights vary in space. In Boston Harbor, the significant change is found along the coasts of inner and outer harbors, with a maximum on the outer shores of the Winthrop Peninsula and Deere Island on the north and Nantasket Peninsula on the south (Fig.11). The SLR's influence will be more significant on the wave height than water elevation. With SLRs from 1.0 to 7.0 ft, the maximum increase values will be in the range of 2 to 13 cm in water elevation and the range of 0.1 to 1.0 m in significant wave height.

In Scituate Harbor, a considerable change of water elevation will occur inside the harbor and on the inner shelf, even though it did show a noticeable increase along the outer coasts of Cedar Point on the north and First to Second Cliffs on the south (Fig.12: upper panel). With SLRs from 1.0 to 7.0 ft, the maximum increase of water elevation will be in the range of 10-30 cm inside the harbor and the inner shelf, while it will be only 15 cm or less along the outer coasts of Cedar Point and Frist Cliff. Over the concave-shaped coast between Frist and Second Cliffs, the increase of water elevation can reach the same order of magnitude as that found inside the harbor. Unlike the water elevation, the significant wave height will increase dramatically along the outer coasts of Cedar Point and First-Second Cliffs, with a maximum occurring in the largest gradient area of the convex-shaped coastline at Cedar Point and First Cliff (Fig.12: lower panel). During the nor'easter, these two areas are the convergence sites of currents driven by northeasterly winds under a condition with the inclusion of wave-current interactions (*Beardsley et al*., 2013; *Chen et al*., 2013).

Meanwhile, when surface waves enter the harbor, they will split into two branches and propagate towards the northwest and southwest ends, respectively. This pattern remains the same for all nor'easter events in the past and even in the cases with SLR. With SLR, the surface waves inside the harbor will be intensified more significantly in the northern branch than in the southern branch. With SLRs from 1.0 to 7.0 ft, the maximum increase of significant wave height will be in the range of 0.2-1.2 m along the outer coast and inside the harbor.

Inundations. For the case without SLR, the total flooding areas were ~32.8 and 0.6 km^2 over the coastal regions of Boston and Scituate Harbors, respectively (Figs.13 and 14). For Boston Harbor, the inundation areas are mainly located around Winthrop Peninsula and Deere Island on the north and Nantasket Peninsula on the south, as well as the western end in the inner harbor (Fig.13). For Scituate Harbor, with surge protection by seawalls along the coast, the flooding usually occurs around the coastal areas inside the harbor, mainly around the coastal area of Cedar Point, shallow shores connected to First Cliff, and the wetland of Rent Street Marshes (Fig.14).

With SLR, the coastal inundation areas will expand inland in Boston Harbor, whereas the Boston city will be vulnerable to flooding (Fig.13). In Scituate Harbor, flooding will become much worse not only around the coastal area inside the harbor and over Rent Street Marshes but also along the coasts of Cedar Point and First to Second Cliff. The coastal area south of Second Cliff will also be extremely vulnerable to extratropical storm-induced flooding (Fig.14).

With SLRs from 1.0 to 7.0 ft, the flooding areas will increase by 1.8, 6.5, 16.4, 33.3, and 100.5% in Boston Harbor and 31.7, 35.0, 50, 58.3, and 113.3% in Scituate Harbor, respectively. In both harbors, the flooding area will enlarge gradually amid SLR of < 5.0 ft (~1.5 m) and rapidly if SLR > 5.0 ft (Fig.15). The 5-ft SLR seems to be a critical level. Over this level, the flooding area can increase exponentially under a hundred-year storm condition.

It should be pointed out here that the inundation maps presented in Figs.13 and 14 do not count the wave runup-produced coastal splashing/overtopping. The increase of significant wave height with SLR implies that the wave runup-produced splashing/ overtopping will become stronger in the future. Using *Allsop et al*. (2005)'s empirical formulas for overtopping across steep seawalls, we estimated the wave runup-produced overtopping discharge in Boston and Scituate Harbors. The assessment was done over the Winthrop Peninsula and Deere Island coast on the north and the Nantasket Peninsula coast on the south in the outer Boston Harbor, and the Cedar Point shore along the outer Scituate area. The overtopping discharges are estimated based on significant wave heights and peak periods on the 20-m isobath off the coast. The SWAVE-predicted surface waves were validated with historical and real-time measurement data recorded on all available NOAA buoys in the U.S. northeastern region (http://134.88.228.119:8080 /fvcomwms/) (*Qi et al*., 2009). A storm buoy was deployed on the 20-m isobath off Scituate Harbor on April 25, 2014, with a week's time coverage period. The SWAVE-predicted significant wave heights and peak periods were validated by comparing the wave records on this buoy.

For the February 1978 nor'easter, the model-predicted wave runup-produced overtopping varied with time. In Boston Harbor, the maximum value was 3.6×10^{3} m^2/s, occurring over the Winthrop Peninsula and Deere Island coast on the north and the Nantasket Peninsula shore on the south. In Scituate Harbor, the maximum value was 0.5×10^3 m^2/s, occurring over the coast of Cedar Point. The total accumulated discharge over February 7-8 was 57.9 km^2 for Boston Harbor and 4.5 km^2 for Scituate Harbor. They were the same order of magnitude or even more significant than the inundation area caused by surges. With SLRs from 1.0 to 7.0 ft, the maximum overtopping discharge rate will increase by 27.9, 54.8, 85.6, 128.2, and 175.4 m^2/s in Boston Harbor and 5.0, 10.1, 14.4, 19.8 and 32.2 m^2/s in Scituate Harbor, respectively (Fig.16). The increase of total overtopping discharges with SLR follows a linear-regression trend (Fig.17).

4. Discussion

The impacts of SLR on the future storm-induced coastal inundation are assessed using a wave-current coupled model of NECOFS. *Chen et al*. (2013) pointed out that the storm-induced coastal inundation over the Mass coast was a fully nonlinear process. The wave and current interaction can significantly enhance the storm-induced onshore water transport. *Beardsley et al*. (2013) found that the onshore flow's intensification can increase the peak of the modeled surge by ~8 cm. Our experiments, made using a wave-current coupled model, showed that the significant wave height varied with water depth during tidal cycles, higher at high tide and lower at low tide. The difference was ~1.0 m at high tide for the cases with and without the inclusion of wave-current interactions (Fig.18). Under the same wind condition, the increase of significant wave height with SLR will be much higher in the case without the inclusion of wave-current interactions (Fig.19). This result suggests that the intensification of surface waves with SLR can be over-projected if wave-current interactions are not taken into account. Since storm surges are directly relevant to the onshore water transport that is significantly influenced by wave-current interactions, a surge prediction may not be accurate enough to meet the stakeholders' expectations if done using a model without the inclusion of wave-current interactions.

In recent years, the wave runup-induced overtopping has become more intense over the U.S. northeast coast, particularly in Boston and Scituate Harbors (Tony Mignone and John Cannon in NOAA, personal communications). We collected the wind and wave records on Buoy#44013 in Mass Bay over 1985-2017 and examined the interannual variability of wave intensity under given wind speeds. We found that for given wind speeds of 5.0, 10.0, 15.0, and 20.0 m/s, the intensity of surface waves exhibited an increasing linear trend in the past 33 years (Fig. 20), with a maximum value of ~2.0 m. This evidence suggests that surface waves have become stronger as a result of SLR. As the SLR continues, the wave runup-produced overtopping will become more critical for coastal inundations in the future.

Bilskie et al. (2014) examined the impacts of SLR on the hurricane-induced storm surge in the Mississippi and Alabama coast. They introduced a normalized nonlinearity (NNL) index given as $(\eta_2 - \eta_1)/\lambda - 1$, where η_1 and η_2 were the maximum surges for the lower and higher sea states with SLR, λ was the difference in maximum surge heights to the amount of SLR. This index provided a spatial distribution of NNL for storm responses to SLR with changes in mean sea level, land use, and land cover.

Differing from the Gulf of Mexico, the GoM is an M_2 tidal resonance region (*Garrett*, 1972; *Brown*, 1984; *Chen et al*., 2011), in which the tidal elevation is much higher than the subtidal elevation. As pointed out by *Greenberg et al*. (2012), in the GoM, "*the determination of changing flood risk over the next century will be more complex than simply adding future contributions determined from climate models*." Tidal energy in the North Atlantic enters the GoM through the Northeast Channel and western Scotian Shelf (Fig. 20). A large fraction of this energy propagates into the Bay of Fundy (BF). At the same time, the rest turns counterclockwise and propagates southwestward along the western GoM towards Massachusetts Bay (MB) (*Chen et al*., 2011). The *Greenberg et al*. (2012)' analysis clearly showed that the modern SLR in the GoM/BF system, attributed in part to post-glacial rebound, has increased the tidal range that is not spatially uniform due to the tidal resonance nature of the GoM/BF system. Using the NECOFS, we assessed the change of amplitude and phase of the M_2 tidal wave in the GoM with SLR. The results supported *Greenberg et al*. (2012)' analysis results. Although no significant increase was found in the M_2 tidal propagation speed, the tidal amplitude change varied significantly in space, especially in BF, the largest tidal resonance region in the GoM. When combined with global-warming-induced SLR, this process will produce even higher high water levels in the future.

Our simulation considered the influence of SLR on tidal waves in the study region. We did see that the maximum surge shifted earlier with SLR. During storm events, the peak surge level was about the same order or even lower than the tidal elevation. In Boston and

Scituate Harbors, the coastal inundation could occur only near or at the high tide (*Chen et al*., 2013). The influence of nonlinearity was mainly due to the wave-current interaction, which enhanced onshore water transports. No efforts were made in this study on the responses of storm-induced coastal inundation to the land use and land cover, like what was accomplished in the Gulf od Merico (*Bilskie et al.,* 2014, 2016; 2019; *Taylor et al., 2015*; *Passeri et al*. 2015, 2016). Similar studies should be considered as our coastal inundation model is expanded to cover a suburb area encompassing intensive saltmarsh where the land cover has been significantly changed due to SLR.

The reliability of the projection for the influence of SLR on the future storm-induced coastal inundation relies on model uncertainties. The uncertainty for our projects was mainly based on RMSE based on the model-data comparison results. In Boston and Scituate Harbors, the model provided an accurate prediction of tidal elevation within an uncertainty range of < 2.0 cm (*Chen et al*., 2013; *Beardsley et al*., 2013). Therefore, the significant RMSE was caused by the predicted intensity and distribution of the storm winds. Since the RMSE caused by weather forcing is nonlinear, the simple RMSE analysis might be too simple to quantify uncertainties due to different dynamics and geometric factors. *Taylor et al*. (2014) developed a computationally efficient uncertainty analysis tool based on an optimal sampling method. This method constructed a storm response function (SRF) on the physical sampling basis. The mean SRF RMSE provides a more physically based objective hazard assessment with SLR. This method was not coded in our coastal inundation model yet, which should be considered in our future studies.

5. Conclusions

The US northeast coastal region has undergone significant SLR, which varies geographically with latitude; higher in New York and lower in the northern Gulf of Maine. Boston and Scituate Harbors in Mass are incredibly vulnerable to extratropical nor'easter-induced flooding. Using a well-validated wave-current coupled FVCOM inundation model of NECOFS, we assessed SLR’s potential impacts on the future extratropical storms-induced coastal inundation in Boston and Scituate Harbors. A series of numerical experiments were made with SLRs from 1.0 to 7.0 ft under a hundred-year storm condition. The results indicate that the influences of SLR on water elevation and surface waves vary significantly in space. In Boston Harbor, more significant changes will be the Winthrop Peninsula and Deere Island coast on the north and the Nantasket Peninsula coast on the south. In Scituate Harbor, the maximum changes will be the Cedar Point coast on the north and First to Second Cliffs on the south. As a result, the inundation areas will enlarge significantly with SLR, with a 5-ft SLR seeming to be a critical level. As SLR > 5 ft, the flooding area can increase exponentially.

The wave runup-produced overtopping has the same order of magnitude as surge-induced flooding. It will become a severe risk for coastal inundation over the US northeast coast as storm-induced surface waves are intensified with sustained SLR.

In Boston and Scituate Harbors, the impacts of SLR on the future storm-induced coastal inundation also exhibited a fully nonlinear dynamical feature required to be assessed using a wave-current coupled model. The surface wave intensification could be over-projected if wave-current interactions are not taken into account. Under the same wind condition, the wave simulation with a coupling of oceanic currents projects a higher increase of significant wave height with SLR compared with the wave-current interaction case. This result suggests that the surface wave intensification could be over-projected if wave-current interactions are not taken into account.

Acknowledgments

This project was supported by the NOAA-funded IOOS NERACOOS program for NECOFS with subcontract numbers NA16NOS0120023 and NERACOOS A007 and the MIT Sea Grant College Program through grants 2012-R/RC-127. Dr. Yu Zhang was supported by the National Natural Science Foundation of China under grant number 41706210 and the National Key Research and Development Programs of China under the grant number 2019YFA0607000. Danya Xu was supported by the Natural Science Foundation of China under grant number U1811464. We would like to thanks Drs. Robert Thompson, John Cannon, Tony Mignone, and Joseph Dellicarpini at NOAA Weather Forecast Office for their valuable suggestions in developing the inundation model.

Disclosure of Potential Conflicts of Interest

Funding: This study was supported by the NOAA-funded IOOS NERACOOS program with subcontract numbers NA16NOS0120023 and NERACOOS A007 and the MIT Sea Grant College Program through grants 2012-R/RC-127.

Conflict of Interest: Dr. Chen has received research grants from the NOAA-funded IOSS NERACOOS Program with subcontract numbers NA16NOS0120023 and NERACOOS A007 and the MIT Sea Grant College Program through grants 2012-R/RC-127. Dr. Yu Zhang was supported by the National Natural Science Foundation of China under grant number 41706210 and the National Key Research and Development Programs of China under the grant number 2019YFA0607000. Danya Xu was supported by the Natural Science Foundation of China under grant number U1811464. Dr. Chen declares that other authors have no conflict of interest.

References

Allsop, W., T. Bruce, J. Pearson, and P. Besley (2005), Wave overtopping at vertical and steep seawalls, *Proceedings of the Institution of Civil Engineers, Maritime Engineering* 158 (MA3), 103-114.

Altimari, D. (1998), Blizzard Of 1978: Feb. 6-7, 1978: The Blizzard Of '78 Shut Down The State And Made Heroes Out Of Those With Four-Wheel Drive", Hartford Courant, February 25, 1998

Beardsley, R. C., C. Chen, and Q. Xu (2013), Coastal flooding in Scituate (MA): a FVCOM study of the Dec. 27, nor'easter*, J. Geophys. Res.-Oceans,* 118, doi: 10.1002/2013 JC008862.

Bernier, N. and K. R. Thompson (2006), Predicting the frequency of storm surges and extreme sea levels in the northwest Atlantic, *J. Geophys. Res*., *111*, C10009, doi:10.1029/2005JC003168.

Bilskie, M. V., S. C. Hagen, S. C. Medeiros, and D. L. Passeri (2014), Dynamics of sea level rise and coastal flooding on a changing landscape, *Geophys. Res. Lett*., 41, 927–934, doi:10.1002/2013GL058759.

Bilskie, M.V., S. C. Hagen, K. Alizad, S. C. Medeiros, D. L. Passeri, H. F. Needham, and A. Cox (2016), Dynamic simulation and numerical analysis of hurricane storm surge under sea level rise with geomorphologic changes along the northern Gulf of Mexico, Earth's Future, 4, 177–193.

Bilskie, M. V., S. C. Hagen, and J. L. Irish (2019), Development of return period stillwater floodplains for the northern Gulf of Mexico under the coastal dynamics of sea level rise, *J. Waterway, Port, Coastal, Ocean Eng*., 145(2), 04019001, doi: 10.1061/(ASCE)WW.1943-5460.0000468.

Brizzolara S., N. Couty, Q. Hermundstad, A. Ioan, T. Kukkanen, M. Viviani, and P. Temarel (2008), Comparison of Experimental and Numerical Loads on an Impacting Bow Section. In: Ships and Offshore Structures, vol. 3; p. 305-324, ISSN: 1744-5302.

Brizzolara S., L. Savio, M. Viviani, Y. Chen. et al. (2011), Comparison of Experimental and Numerical Sloshing Loads in Partially Filled Tanks. In: Ships and Offshore Structures, vol. 6, pp. 15-43, ISSN: 1744-5302.

Brown W. S. (1984), A comparison of Georges Bank, Gulf of Maine and New England Shelf tidal dynamics, *Journal of Physical Oceanography*, 14, 145-167.

Burchard, H., (2002), Applied turbulence modeling in marine waters. *Springer: Berlin-Heidelberg-New York-Barcelona-Hong Kong-London-Milan Paris-Tokyo*, 215pp.

Chen, C., H. Liu and R. Beardsley (2003), An unstructured grid, finite-volume, three dimensional, primitive equations ocean model: Application to coastal ocean and estuaries, *J. Atm. & Ocean Tech*., *20 (1)*, 159–186.

Chen, C, R. C. Beardsley and G. Cowles (2006a), An unstructured grid, finite-volume coastal ocean model (FVCOM) system, Special Issue entitled "Advances in Computational Oceanography", *Oceanography*, *19(1)*, 78-89.

Chen, C, G. Cowles and R. C. Beardsley (2006b), An unstructured-grid, finite-volume coastal ocean model: FVCOM User Manual, Second Edition, *SMAST/UMASSD Technical Report*-06-0602, pp 315

Chen, C, J. Qi, C. Li, R. C. Beardsley, H. Lin, R. Walker and K. Gates (2008), Complexity of the flooding/drying process in an estuarine tidal-creek salt-marsh system: an application of FVCOM, *J. Geophys. Res*.-*Oceans*, 113, C07052doi: 10.1029/2007 JC004328.

Chen, C., H. Huang, R. C. Beardsley, Q. Xu, R. Limeburner, G. W. Cowles, Y. Sun, J. Qi, and H. Lin (2011), Tidal dynamics in the Gulf of Maine and New England Shelf: An application of FVCOM, *J. Geophys. Res*.-*Oceans*, 116, C12010, doi:10.1029 /2011JC007054.

Chen, C. R. C. Beardsley, R. A Luettich Jr, J. J. Westerink, H. Wang, W. Perrie, Q. Xu, A. S. Dohahue, J. Qi, H. Lin, L. Zhao, P. Kerr, Y. Meng and B. Toulany (2013), Extratropical storm inundation testbed: intermodal comparisons in Scituate, Massachusetts, *J. Geophys. Res.-Oceans,* 118, doi:10.1002/jgrc.20397.

Chen, C., R. C. Beardsley, G. Cowles, J. Qi, Z. Lai, G. Gao, D. Stuebe, H. Liu, Q. Xu, P. Xue, J. Ge, R. Ji, S. Hu, R. Tian, H. Huang, L. Wu, H. Lin, Y. Sun, L. Zhao (2013a), An unstructured-grid, finite-volume community ocean model FVCOM user manual (3rd edition), *SMAST/UMASSD Technical Report-13-0701*, University of Massachusetts-Dartmouth, pp 404.

Dudhia, J., and J.F. Bresch (2002), A global version of the PSU-NCAR Mesoscale Model, *Mon. Wea. Rev., 130-12*, 2989-3007, doi: 10.1175/1520-0493(2002)130.

Dudhia et al. (2003), A nonhydrostatic version of the Penn State/NCAR mesoscale model: Validation tests and simulation of an Atlantic cyclone and cold front, *Mon. Wea. Rev*., 121,1493–1513.

Earls, A. R., and M. S. Dukakis (2008), Greater Boston's Blizzard of 1978, Arcadia Publishing, 2008, ISBN 978-0-7385-5519-5.

Freedman, A. (2010), Blizzard blasts coastal cities from Va. to Mass, *The Washington Post-December 27, 2010.*

Freedman, A. (2013), Blizzard of 2013 brings another threat: coastal flooding, *Climate Central News* published on February 8, 2013.

Garrett, 1972. Tidal resonance in the Bay of Fundy and the Gulf of Maine, Nature, 238 (5365), 441-443.

Gómez-Gesteira, M., B. D. Rogers, A. J. C. Crespo, R. A. Dalrymple, M. Narayanaswamy, and J. M. Dominguez (2012a) "SPHysics - development of a free-surface fluid solver- Part 1: Theory and Formulations". *Computers & Geosciences*, 48, 289-299.

Gómez-Gesteira, M, A. J. C. Crespo, B. D. Rogers, R. A. Dalrymple, J. M. Dominguez (2012), "SPHysics - development of a free-surface fluid solver- Part 2: Efficiency and test cases". *Computers & Geosciences*, 48, 300-307.

Hellmer, H. H., F. Kauker, R. Timmermann, J. Determann, and J. Rae (2012.), Twenty-first-century warming of a large Antarctic ice-shelf cavity by a redirected coastal current, *Nature*, 485, 225-228.

IPCC (2007), Climate Change 2007: The Physical Science Basis. Contribution of Working Group I to the Fourth Assessment Report of the Intergovernmental Panel on Climate Change [Solomon, S., D. Qin, M. Manning, Z. Chen, M. Marquis, K.B. Averyt, M.Tignor, and H.L. Miller (eds.)]. Cambridge University Press, Cambridge, United Kingdom and New York, NY, USA.

Lai, Z., C. Chen, G. Cowles, and R. C. Beardsley (2010a), A Non-Hydrostatic Version of FVCOM, Part I: Validation Experiments, *J. Geophys. Res.-Oceans,* 115, doi:10. 1029/2009JC005525.

Lai, Z., C. Chen, G. Cowles, and R. C. Beardsley (2010b), A Non-Hydrostatic Version of FVCOM, Part II: Mechanistic Study of Tidally Generated Nonlinear Internal Waves in Massachusetts Bay, *J. Geophys. Res.-Oceans,* 115, doi: 10.1029/2010 JC006331.

Lin, N., K. Emanuel, M. Oppenheimer and E. Vanmarcke (2012), Physical based assessment of hurricane surge threat under climate change, *Nature Climate Change*, 2, 462-467, doi: 10.1038/ncclimate1389

McCown, S (2008), "Perfect Storm" Damage Summary." *National Climatic Data Center*. National Oceanic and Atmospheric Administration. http://www.ncdc.noaa.gov/oa /satellite/satelliteseye/cyclones/pfctstorm91/pfctstdam.html

Mignone, A., H. Stockdon, M. Willis, J. Cannon, and R. Thompson (2012), On the Use of Wave Parameterizations and a Storm Impact Scaling Model in National Weather Service Coastal Flood and Decision Support Operations,[abs.]: American Meteorological Society Annual Meeting, 92nd, New Orleans, La., January 22–26, 2012; [http://ams.confex.com/ams /92Annual/webprogram/Paper196615.html].

Passeri, D. L., S. C. Hagen, S. C. Medeiros, M. V. Bilskie, K. Alizad, and D. Wang (2015a), The dynamic effects of sea level rise on low-gradient coastal landscapes: A review, *Earth's Future*, 3, 159–181, doi:10.1002/2015EF000298.

Passeri, D. L., S. C. Hagen, M. V. Bilskie, and S. C. Medeiros (2015b), On the significance of incorporating shoreline changes for evaluating coastal hydrodynamics under sea level rise scenarios, *Natural Hazards*, 75: 1599-1617, doi:10.1007/s11069-014-1386-y.

Passeri, D. L., S. C. Hagen, N. G. Plant, M. V. Bilskie, S. C. Medeiros, and K. Alizad (2016), Tidal hydrodynamics under future sea level rise and coastal morphology in the Northern Gulf of Mexico, *Earth's Future*, 4, 159–176, doi:10.1002/2015EF 000332.

Pritchard, H. D., S. R. M. Ligtenberg, H. A. Fricker, D. G. Vaughan, M. R. van den Broeke and L. Padman (2012), Antarctic ice-sheet loss driven by basal melting of ice shelves. *Nature*, 484, 502-505.

Qi, J., C. Chen, R. C. Beardsley, W. Perrie, Z. Lai, and G. Cowles (2009), An unstructured-grid finite-volume surface wave model (FVCOM-SWAVE): implementation, validations, and applications. *Ocean Modelling*, 28, 153-166. doi:10.1016/ j.ocemod.2009.01.007.

Rahmstorf, S. (2010), A new view on sea level rise, *Nature*, 4, 44-45.

Smagorinsky, J. (1963), General circulation experiments with the primitive equations, I. The basic experiment, *Mon. Wea. Rev.*, 91, 99–164.

Sun, Y., C. Chen, R. C. Beardsley, Q. Xu, J. Qi, and H. Lin (2013), Impact of current-wave interaction on storm surge simulation: A case study for Hurricane Bob. *J. Geophys. Res.-Oceans,* 118, 2685-2701, doi:10.1002/jgrc.20207

Taylor, N. R., J. L. Irish, I. E. Udoh, M. V. Bilskie, and S. C. Hagen (2015), Development and uncertainty quantification of hurricane surge response function for hazard assessment in coastal bays, *Natural Hazards*, 77, 1103-1123, doi: 10.1007/s 11069-015-1646-5.

Wu, L, C. Chen, F. Guo, M. Shi, J. Qi and J. Ge (2010), A FVCOM-based unstructured grid wave, current, sediment transport model, I. model description and validation, *J. Ocean. Univ. China,* 10(1): 1-8, doi: 10.1007/s11802-011-1788-3.

Zhao, L., C. Chen, J. Vallino, C. Hopkinson, R. C. Beardsley, H. Lin, and J. Lerczak (2010), Wetland-Estuarine-Shelf Interactions in the Plum Island Sound and Merrimack River in the Massachusetts Coast. *J. Geophys. Res.-Oceans*, 115, C10039, doi:10.1029/2009JC006085.

Figure Captions

Figure 1: Bathymetry of Mass Bay (MB) with enlarged views in Boston and Scituate Harbors. Blue curvature lines in enlarged left up and low panels are the coasts where the wave run-up overtopping is calculated. The red filled triangle is the location of NOAA Buoy#44013. The red filled dot is the location of the tidal gauge.

Figure 2: Projected mean sea level rise over the New England coast from New York on the south to Halifax. The figure was drawn based on the projection of the mean sea level at tidal gauges.

Figure 3: The horizontal FVCOM grids of Scituate and Boston Harbors that are nested with the NECOFS regional FVCOM model. An example of an enlarged view of the model grid over the land and rivers is given in the lower panel. The horizontal resolution is up to ~10 m inside harbors and over the land.

Figure 4: Storm return high water level versus return period summarized from the data recording at NOAA Buoy#44013 and tidal gauge in Boston Harbor before 2015.

Figure 5: Time series of wind vector and air pressure (red line) at NOAA Buoy#44013 over February 5-10, 1978 (based on the model prediction) and August 18-22, 1991 (based on the measurement records).

Figure 6: Comparisons of the observed and simulated total (upper) and storm surge (lower) elevations at the tidal gauge site in Boston Harbor over February 1-8, 1978 (left), and August 16-21, 1991 (right).

Figure 7: Comparisons of observed and simulated air pressures (P_{air}), wind speeds (W_s), wind directions (W_{dir}), significant wave heights (H_s), and peak periods (T_p) at NOAA Buoy#44013 over August 18-21, 1978.

Figure 8: Distributions of the surface elevation (left) and significant wave height (right) in Boston Harbor at 16:00 GMT, February 7, 1978, and 22:00 GMT, August 19, 1991.

Figure 9: Distributions of near-surface water velocities in Boston Harbor at 15: 00 GMT, February 7, and 19:00 GMT, August 19, 1991, respectively.

Figure 10: Distributions of the near-surface water velocity (left) at 13:00 GMT, surface elevation (middle), and significant wave height (right) at 16:00 GMT, February 7, 1978, in Scituate Harbor.

Figure 11: Differences of the surface elevation ($\Delta\zeta$) and significant wave height (ΔH_s) relative to ζ and H_s from the case with SLR = 0.0 for the cases with SLR of 1, 2, 3 5, and 7 ft in Boston Harbor.

Figure 12: Differences of the surface elevation ($\Delta\zeta$) and significant wave height (ΔH_s) relative to ζ and H_s from the case with SLR = 0.0 for the cases with SLR of 1, 2, 3 5, and 7 ft in Scituate Harbor, respectively.

Figure 13: Inundation maps over the Boston Harbor's coast for the cases with SLR of 1, 2, 3, 5, and 7 ft, respectively.

Figure 14: Inundation maps over Scituate Harbor's coast for the cases with SLR of 1, 2, 3, 5, and 7 ft, respectively.

Figure 15: Changes in the flooding area with SLR over the coasts of Boston and Scituate Harbors. Note: the wave runup-produced overtopping is not taken into account.

Figure 16: Differences of the overtopping discharge relative to the value for the case with SLR = 0.0 for the cases with SLR of 1, 2, 3, 5, and 7 ft. Left: Boston Harbor, right: Scituate Harbor.

Figure 17: Changes of overtopping with SLR over the coasts of Boston and Scituate Harbors, respectively. Black: Boston Harbor; red: Scituate Harbor.

Figure 18: Changes of the significant wave height with SLR over the Winthrop Peninsula coast under the conditions without and with the inclusion of wave-current interactions.

Figure 19: Changes of the significant wave height difference (relative to the value for the case without SLR) with SLR over the Winthrop Peninsula coast under the conditions without and with the inclusion of wave-current interactions.

Figure 20: Interannual variability of the significant wave height under given wind speeds of 5, 10, 15, and 20 m/s over 1985-2017, respectively.

Figure 21: Map of the M_2 tidal energy flux vectors in the Gulf of Maine predicted by the NECOFS. MB: Mass Bay, NEC: Northeast Channel.

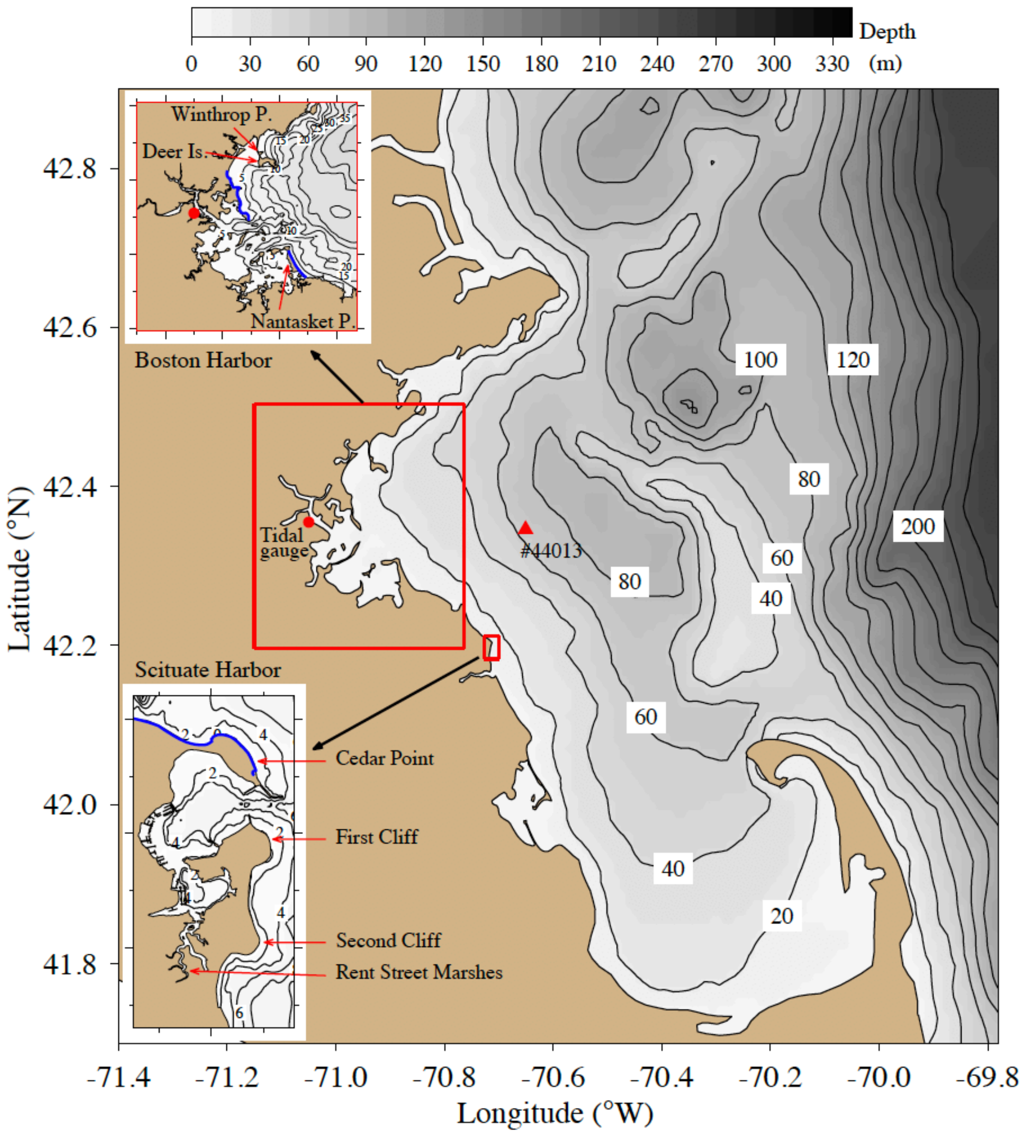

Fig.1: Bathymetry of Mass Bay (MB) with enlarged views in Boston and Scituate Harbors. Blue curvature lines in enlarged left up and low panels are the coasts where the wave run-up overtopping is calculated. The red filled triangle is the location of NOAA Buoy#44013. The red filled dot is the location of the tidal gauge.

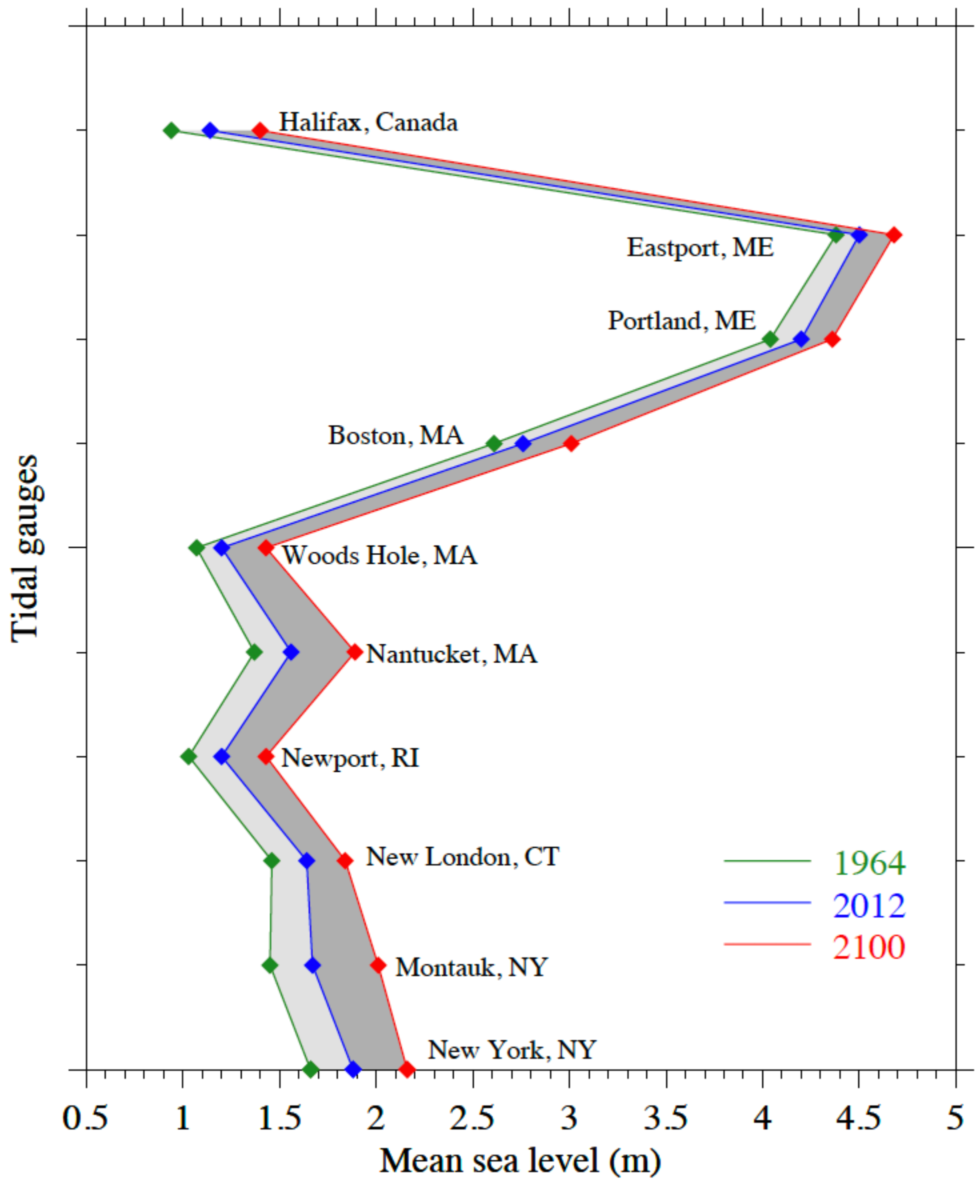

Fig.2: Projected mean sea level rise over the New England coast from New York on the south to Halifax. The figure was drawn based on the projection of mean sea level at tidal gauges.

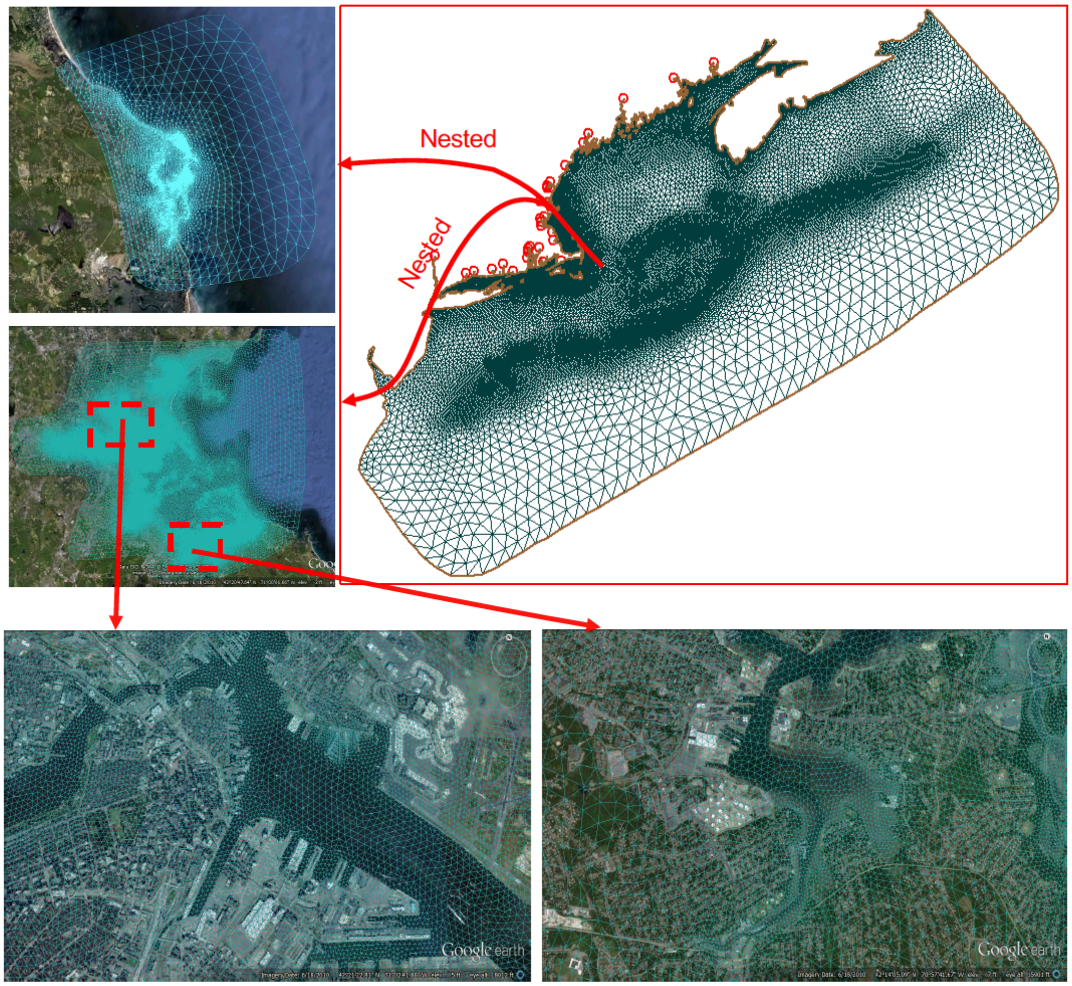

Fig.3: The horizontal FVCOM grids of Scituate and Boston Harbors that are nested with the NECOFS regional FVCOM model. An example of an enlarged view of the model grid over the land and rivers is given in the lower panel. The horizontal resolution is up to ~10 m inside harbors and over the land.

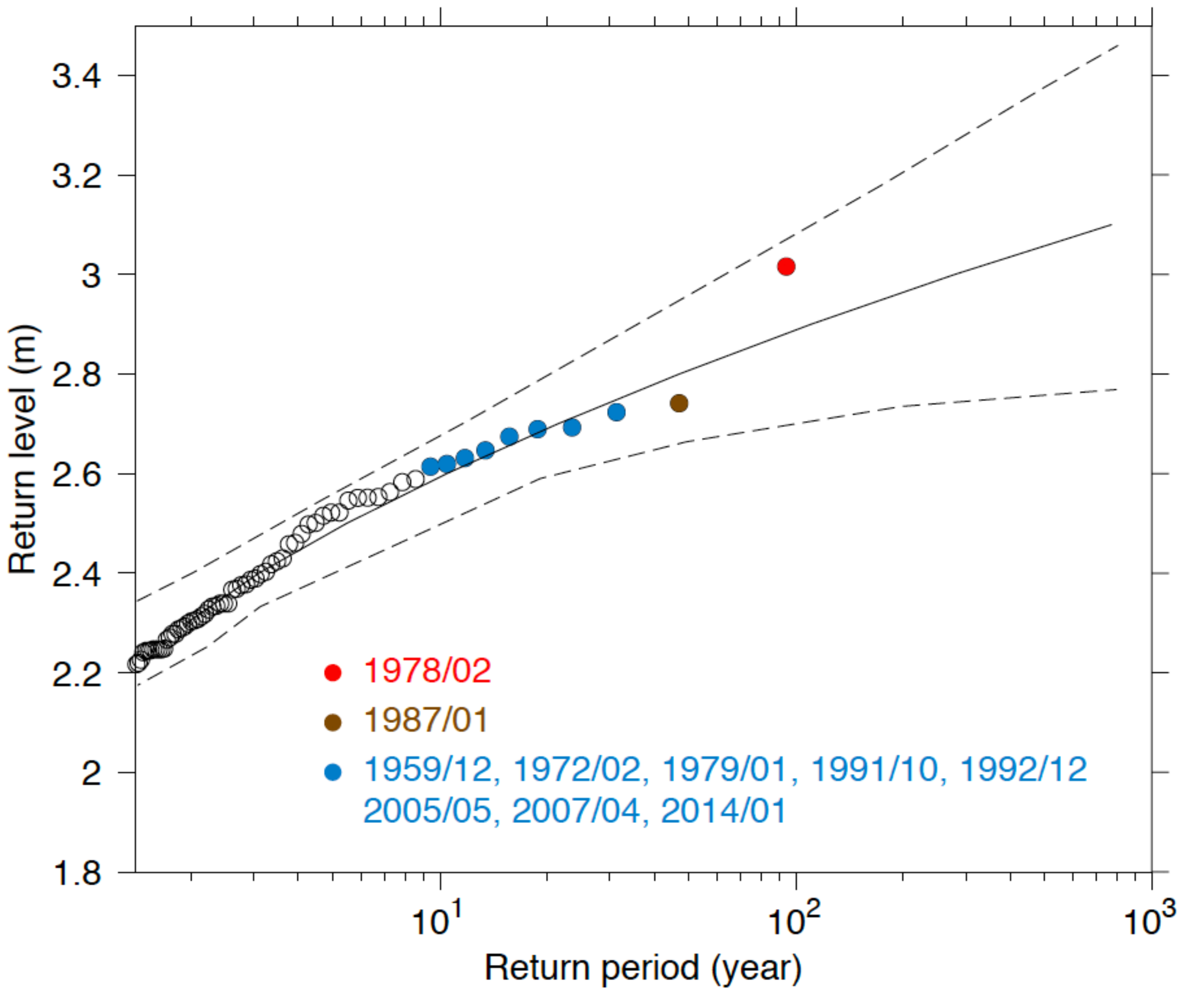

Fig.4: Storm return high water level versus return period summarized from the data recording at NOAA buoy#44013 and tidal gauge in Boston Harbor before 2015.

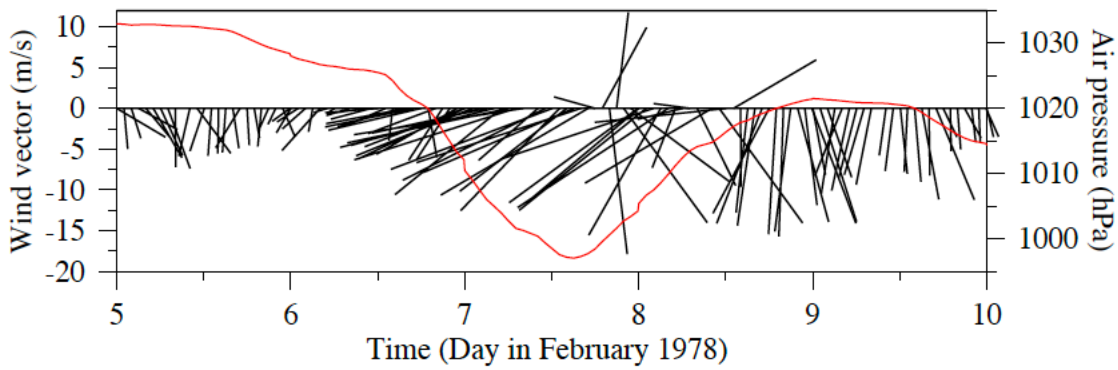

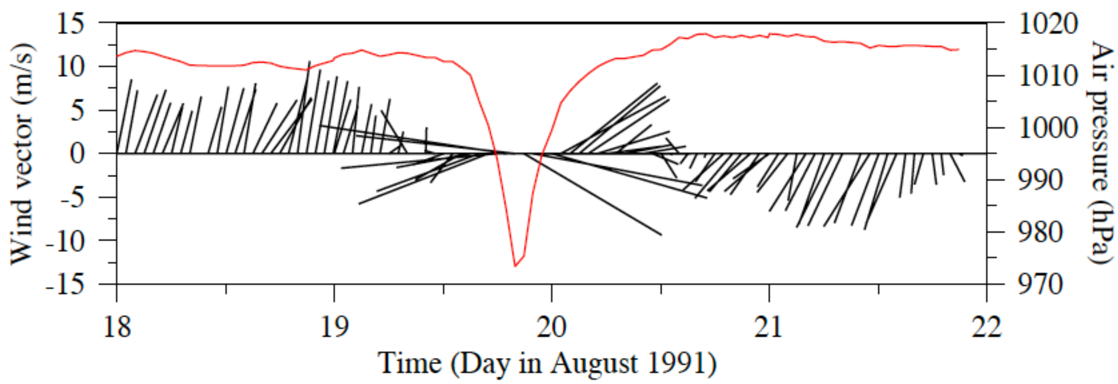

Fig.5: Time series of wind vector and air pressure (red line) at NOAA Buoy#44013 over February 5-10, 1978 (based on the model prediction) and August 18-22, 1991 (based on the measurement records).

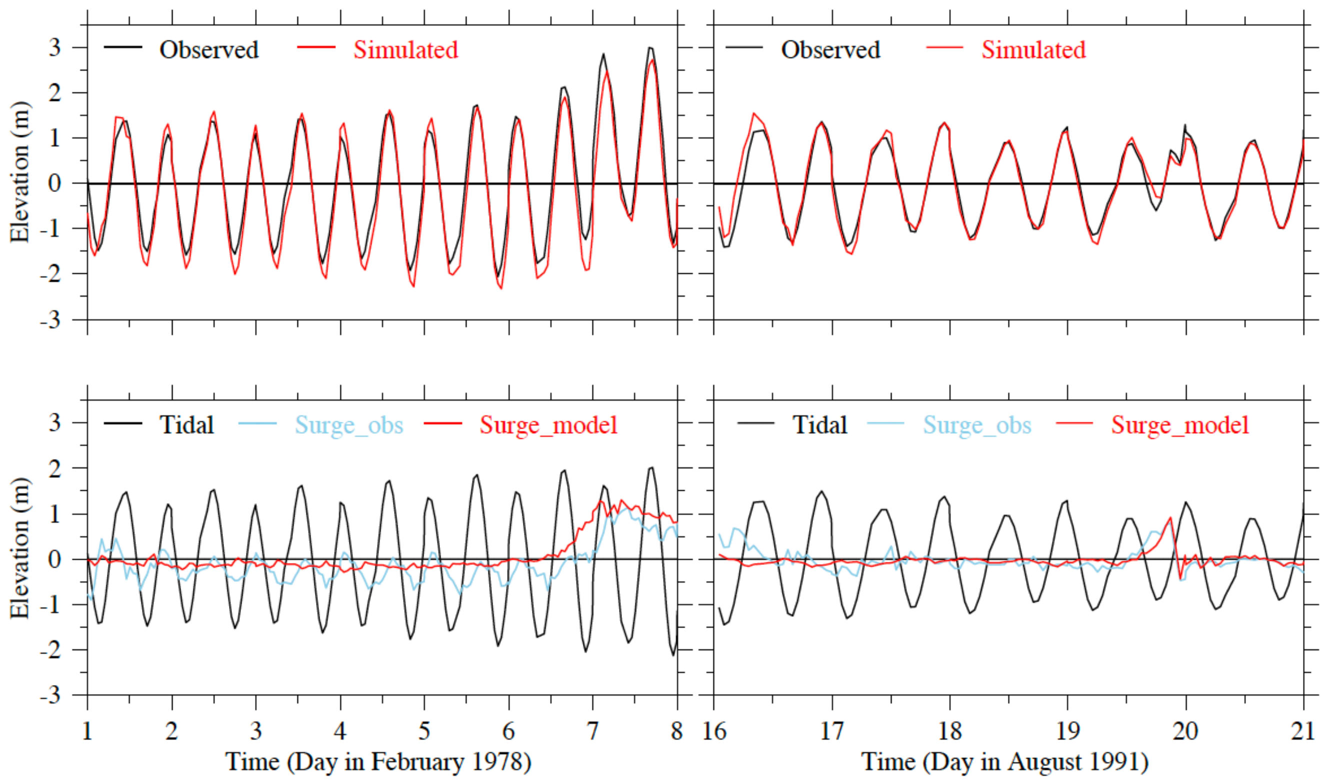

Fig.6: Comparisons of observed and simulated total (upper) and storm surge (lower) elevations at the tidal gauge site in Boston Harbor over February 1-8, 1978 (left) and August 16-2, 1991 (right).

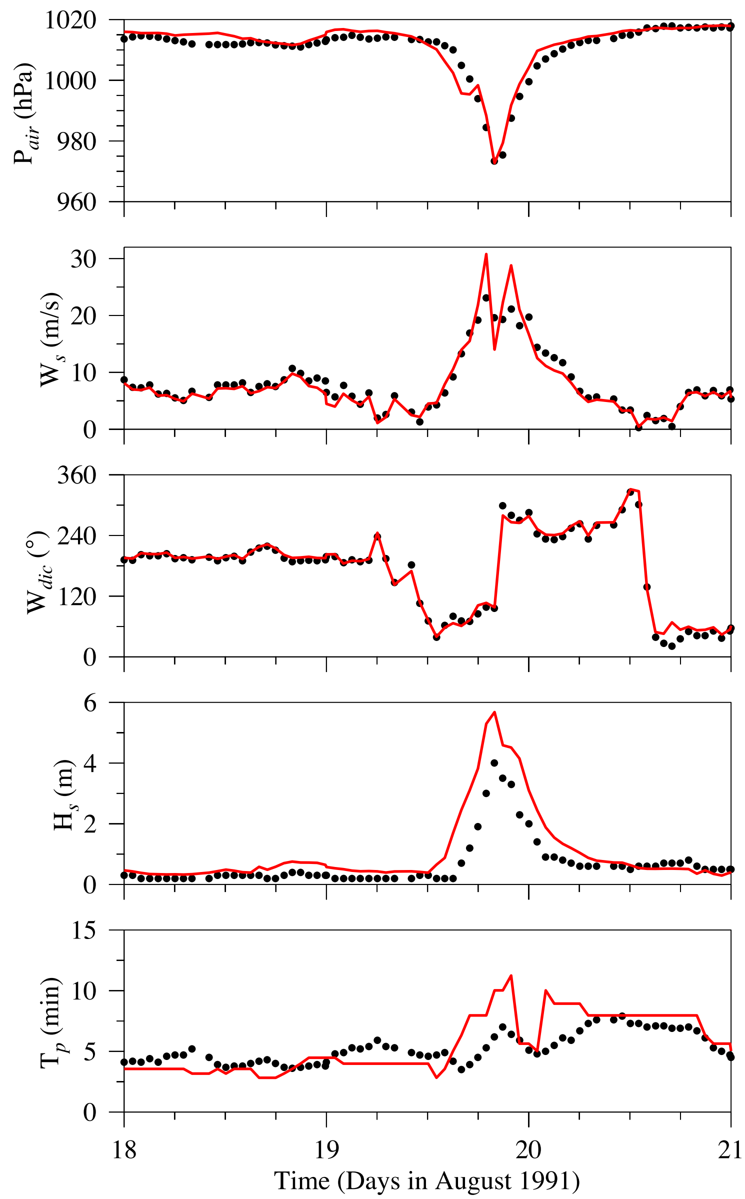

Fig.7: Comparisons of observed and simulated air pressures (P_{air}), wind speeds (W_s), wind directions (W_{dir}), significant wave heights (H_s), and peak periods (T_p) at NOAA Buoy#44013 over August 18-21, 1978.

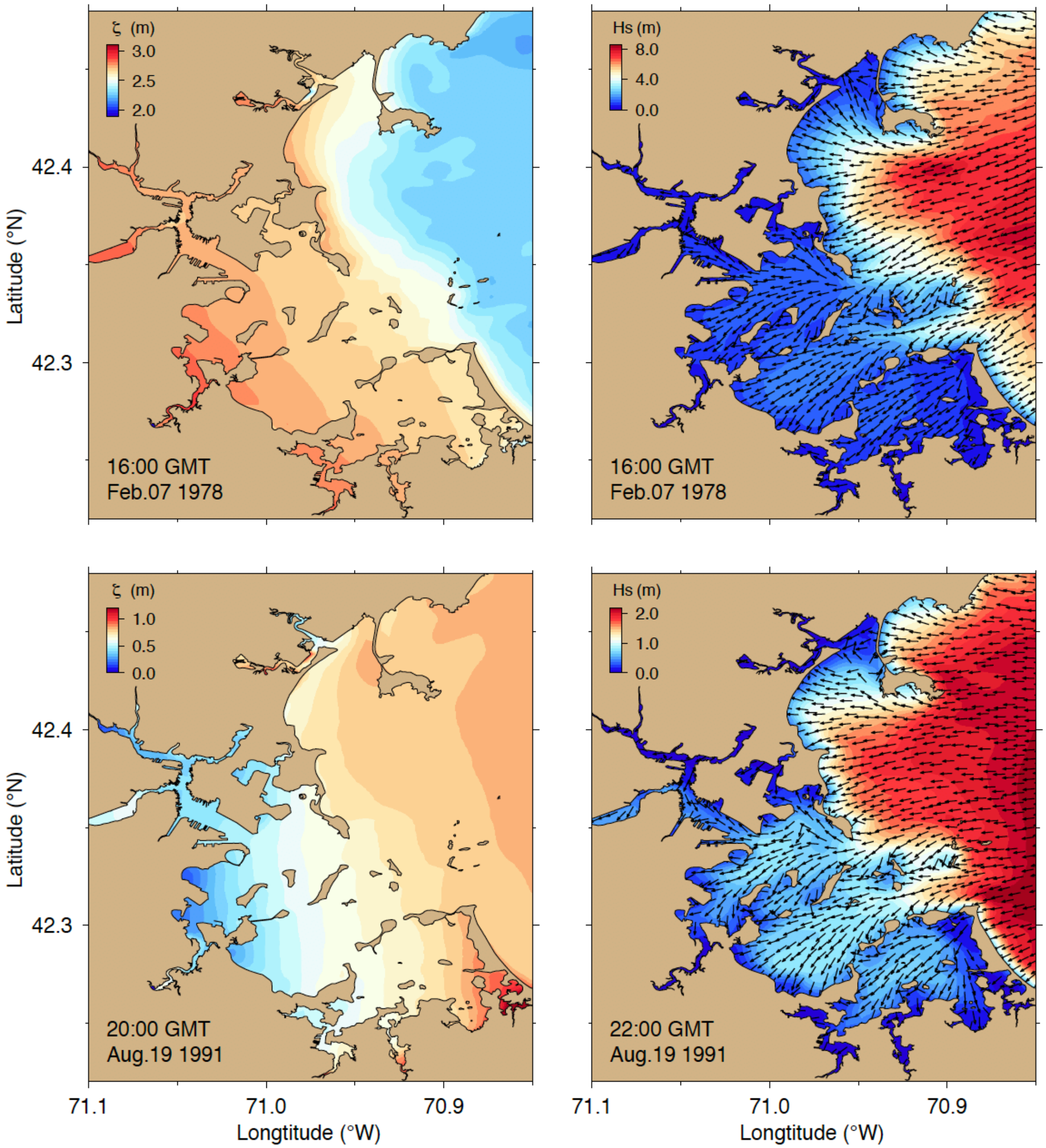

Fig.8: Distributions of the surface elevation (left) and significant wave height (right) in Boston Harbor at 16:00 GMT, February 7, 1978, and 22:00 GMT, August 19, 1991.

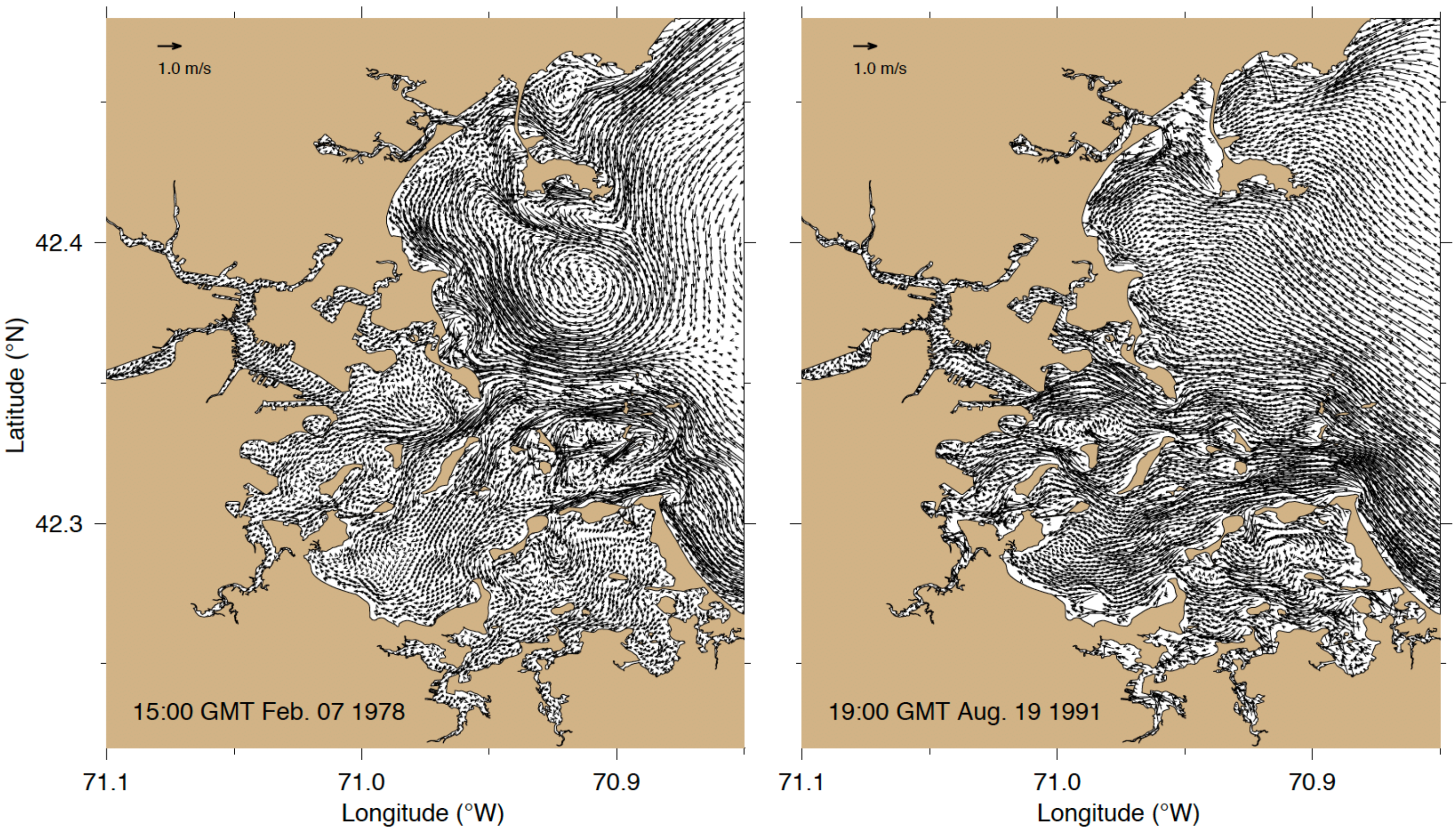

Fig.9: Distributions of near-surface water velocities in Boston Harbor at 15: 00 GMT, February 7 and 19:00 GMT, August 19, 1991, respectively.

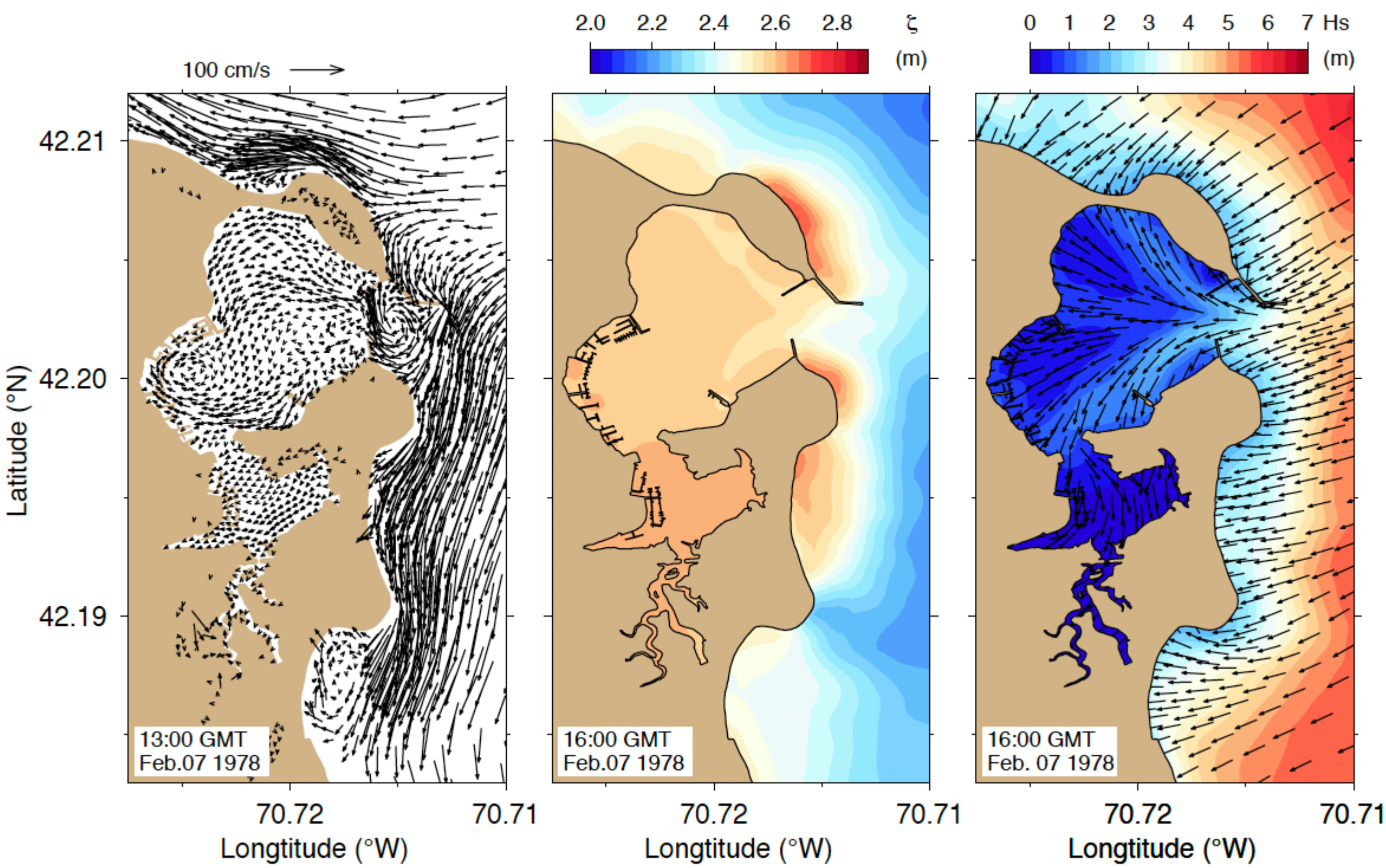

Fig.10: Distributions of the near-surface water velocity (left) at 13:00 GMT, surface elevation (middle), and significant wave height (right) at 16:00 GMT, February 7, 1978, in Scituate Harbor.

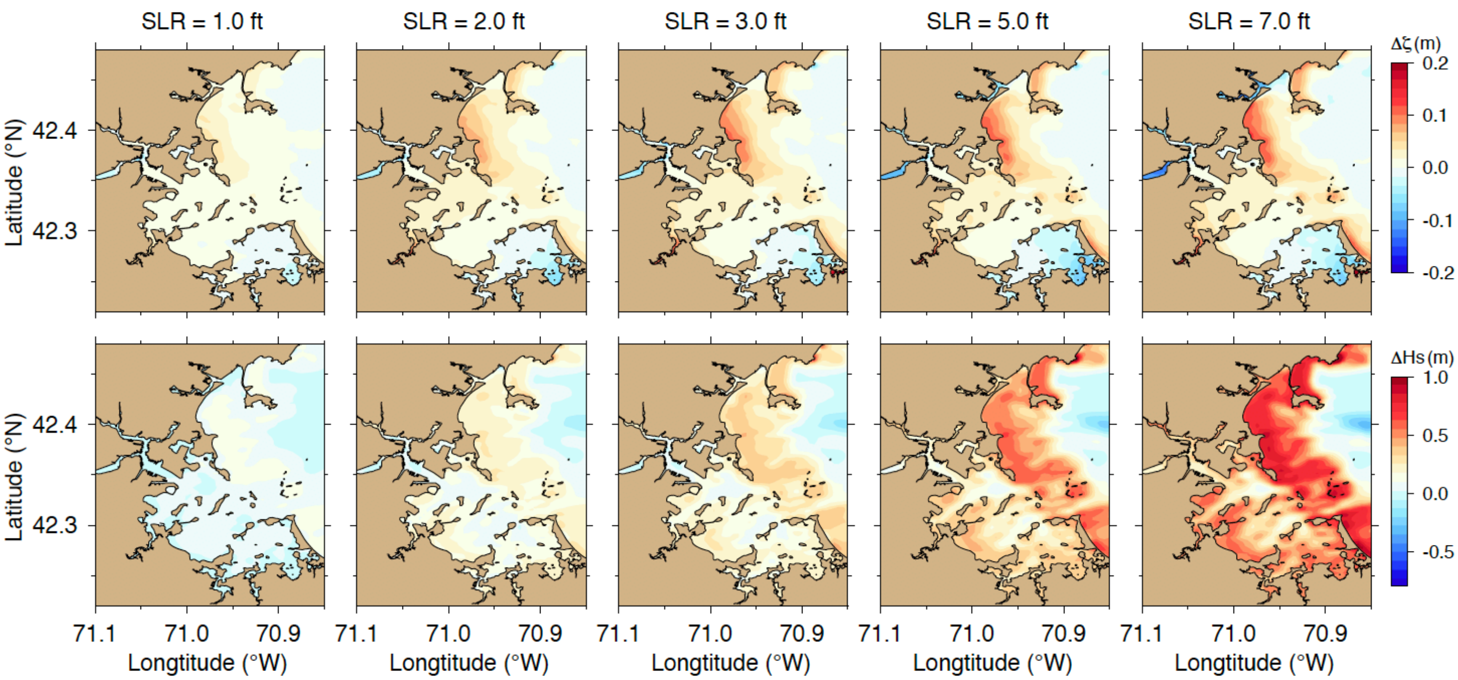

Fig.11: Differences of the surface elevation ($\Delta\zeta$) and significant wave height (ΔH_s) relative to ζ and H_s from the case with SLR = 0.0 for the cases with SLR of 1, 2, 3 5, and 7 ft in Boston Harbor.

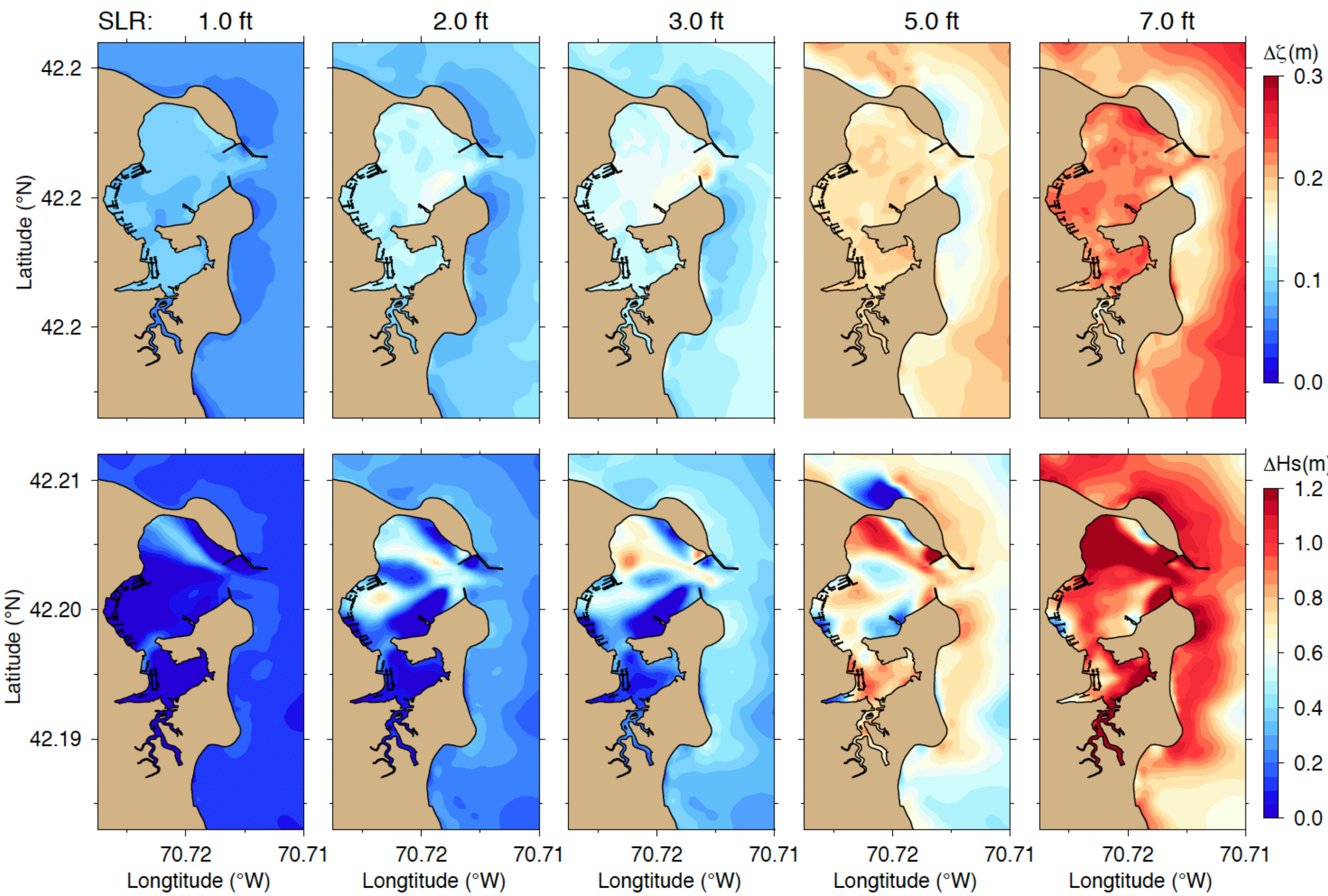

Fig.12: Differences of the surface elevation ($\Delta\zeta$) and significant wave height (ΔH_s) relative to ζ and H_s from the case with SLR = 0.0 for the cases with SLR of 1, 2, 3 5, and 7 ft in Scituate Harbor, respectively.

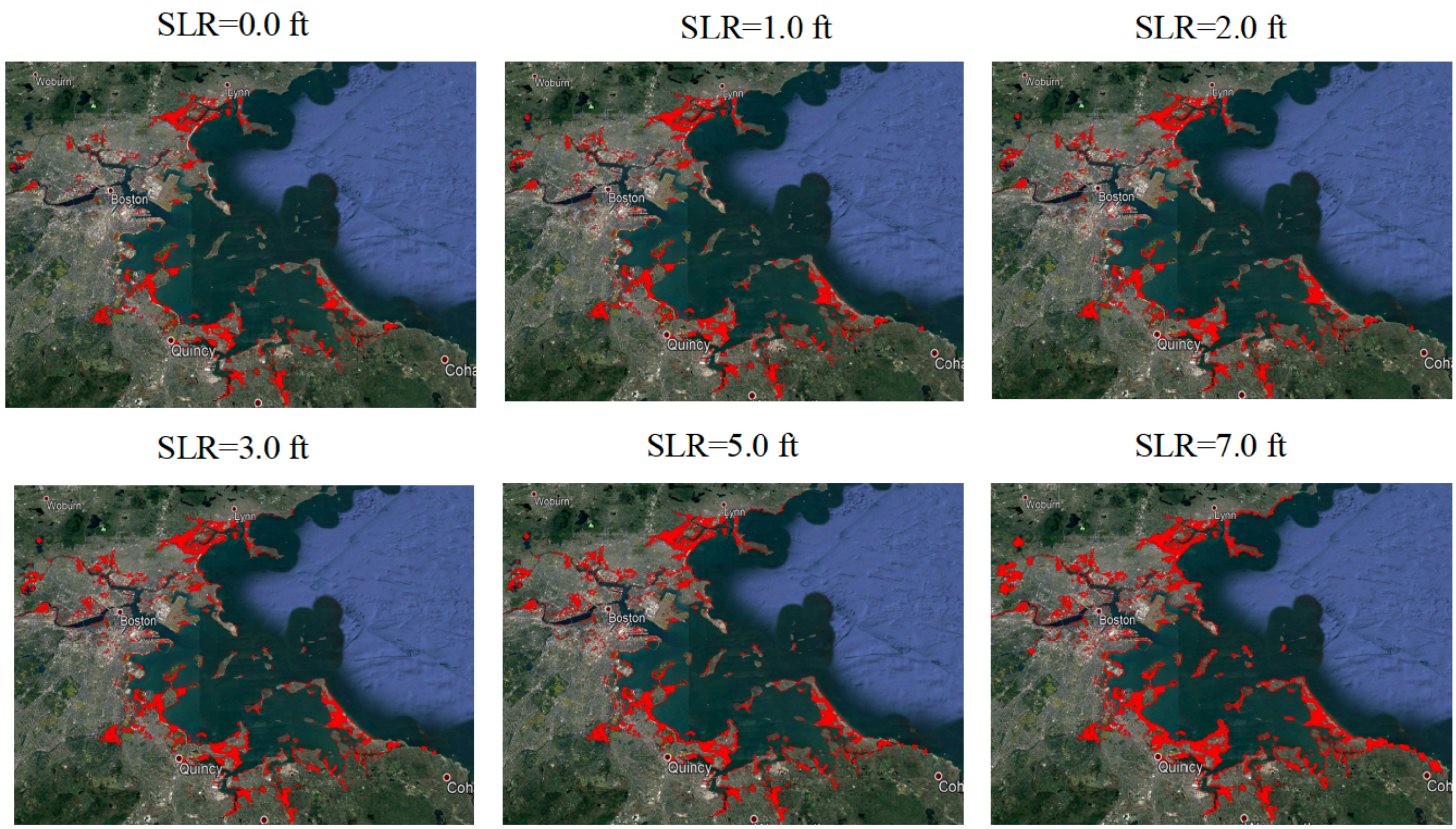

Fig.13: Inundation maps over the Boston Harbor’s coast for the cases with SLR of 1, 2, 3, 5, and 7 ft, respectively.

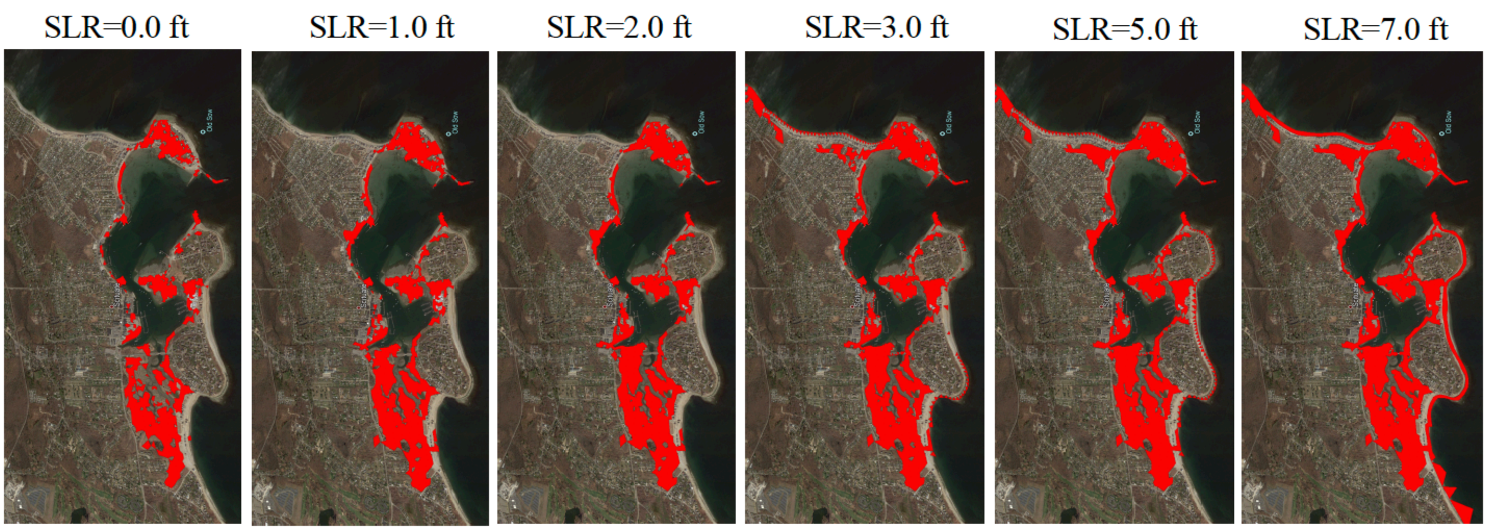

Fig.14: IInundation maps over Scituate Harbor's coast for the cases with SLR of 1, 2, 3, 5, and 7 ft, respectively.

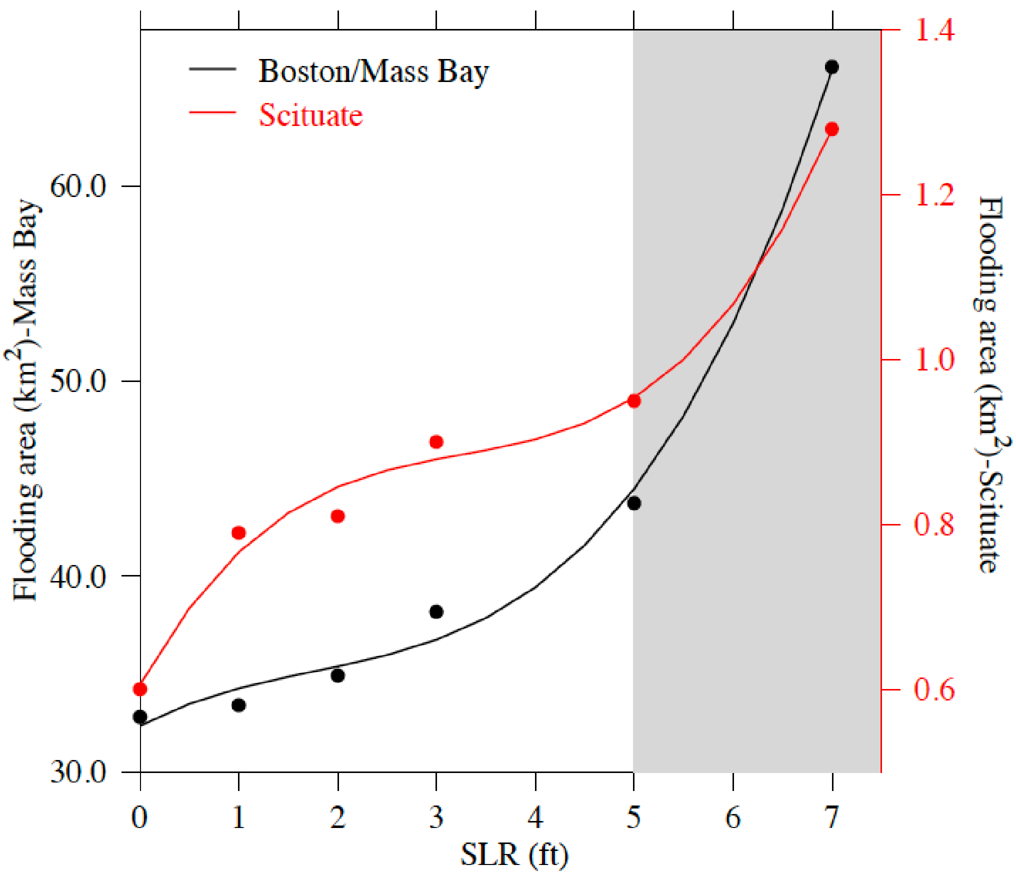

Fig.15: Changes in the flooding area with SLR over the coasts of Boston and Scituate Harbors. Note: the wave runup-produced overtopping is not taken into account. C

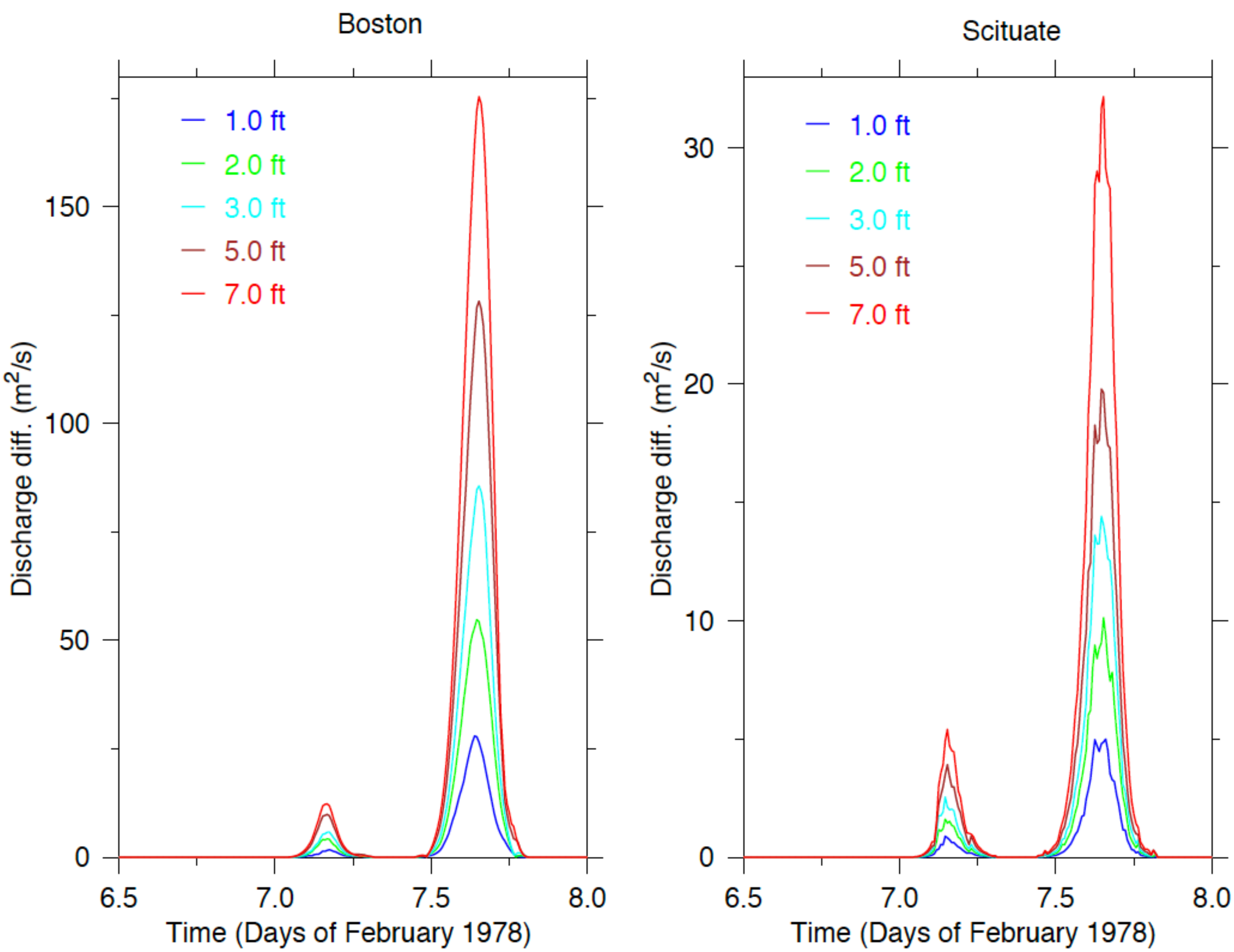

Fig.16: Differences of the overtopping discharge relative to the value for the case with SLR = 0.0 for the cases with SLR of 1, 2, 3, 5, and 7 ft. Left: Boston Harbor, right: Scituate Harbor.

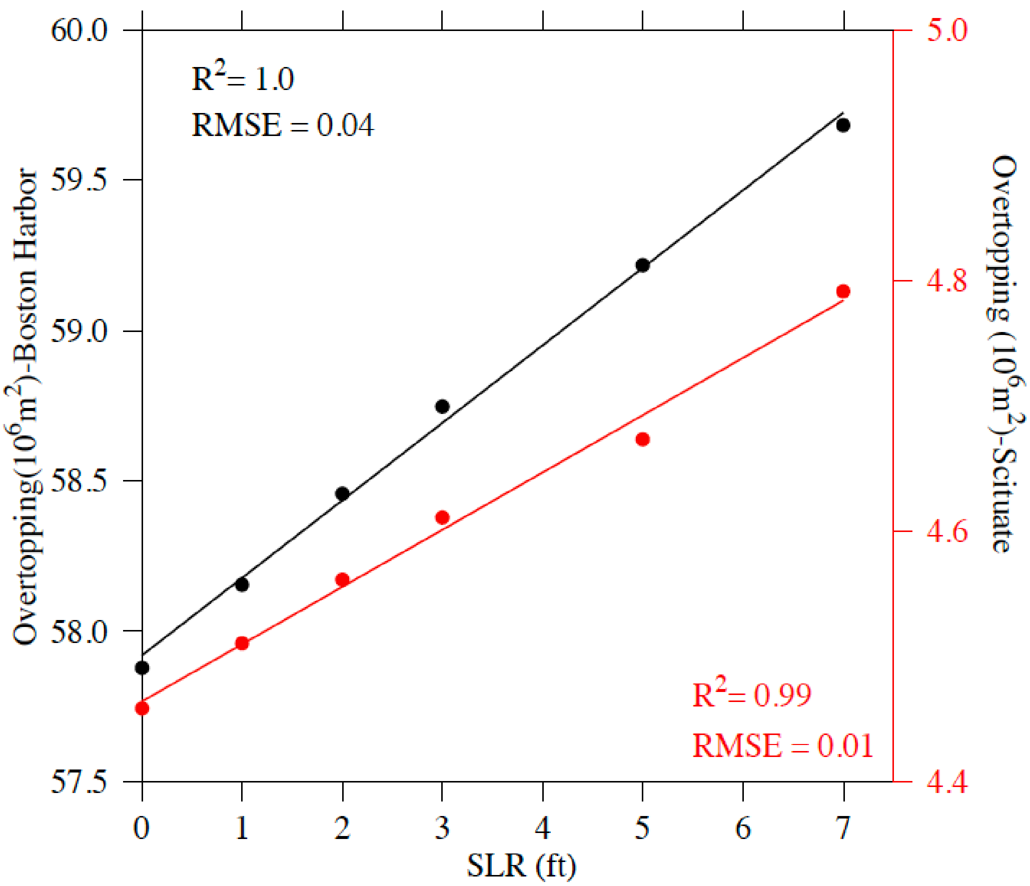

Fig.17: Changes of overtopping with SLR over the coasts of Boston and Scituate Harbors, respectively. Black: Boston Harbor; red: Scituate Harbor.

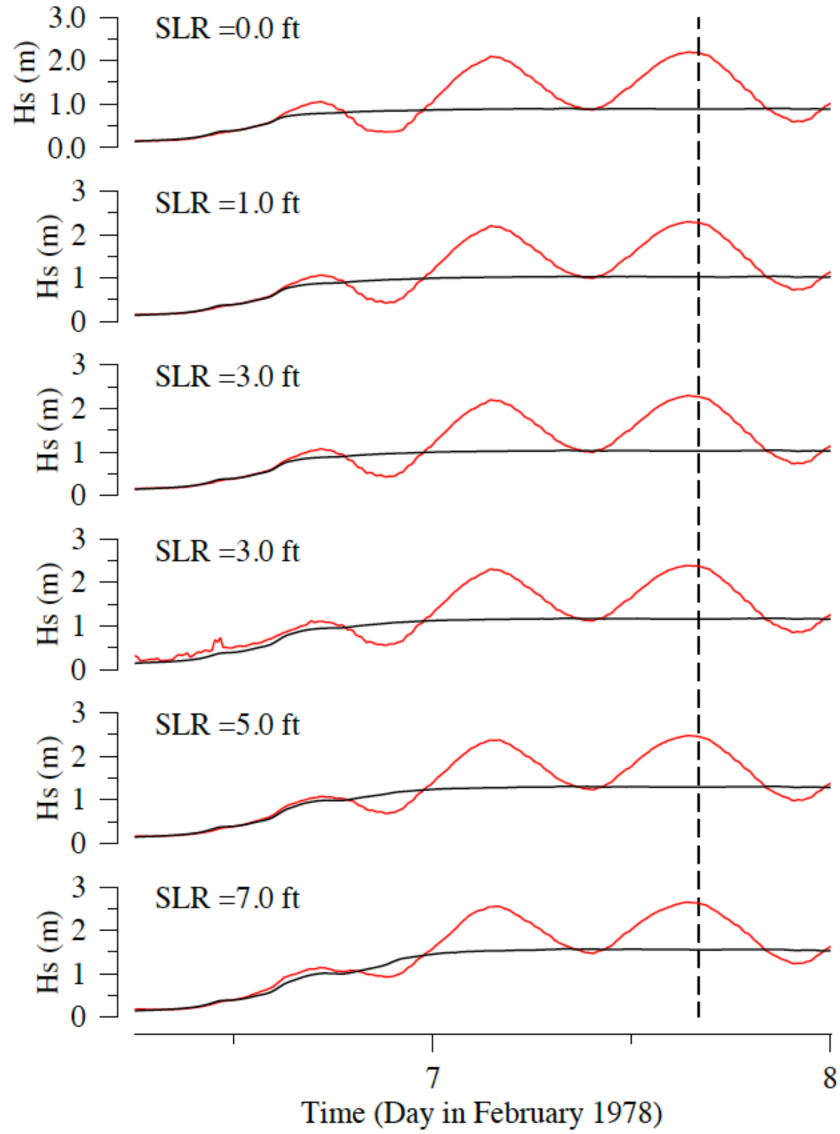

Fig.18: Changes of the significant wave height with SLR over the Winthrop Peninsula coast under the conditions without and with the inclusion of wave-current interactions.

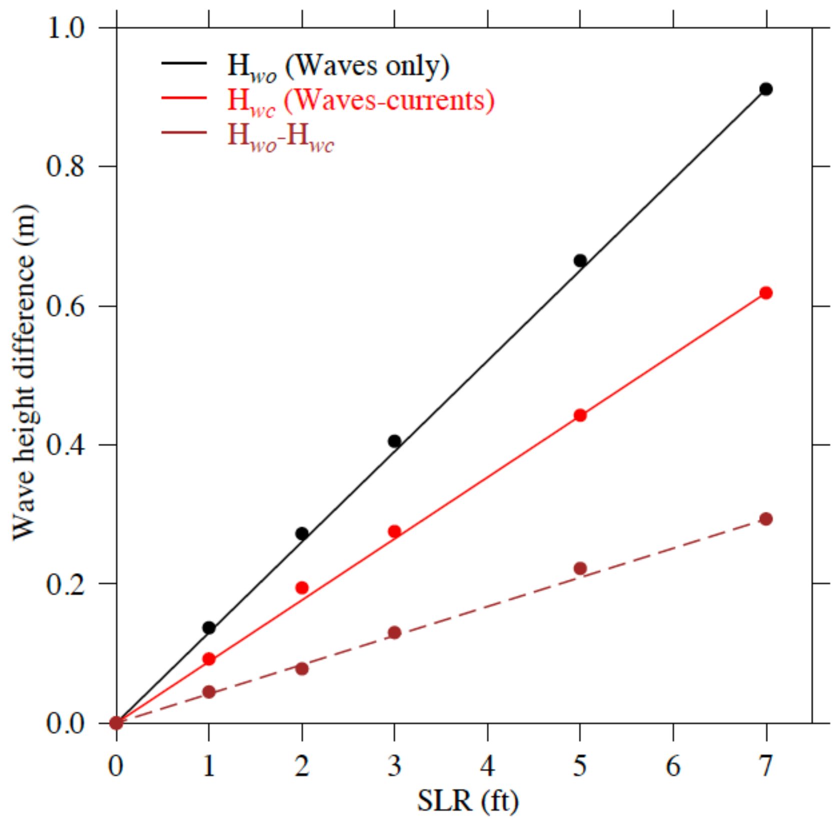

Fig.19: Changes of the significant wave height difference (relative to the value for the case without SLR) with SLR over the Winthrop Peninsula coast under the conditions without and with the inclusion of wave-current interactions.

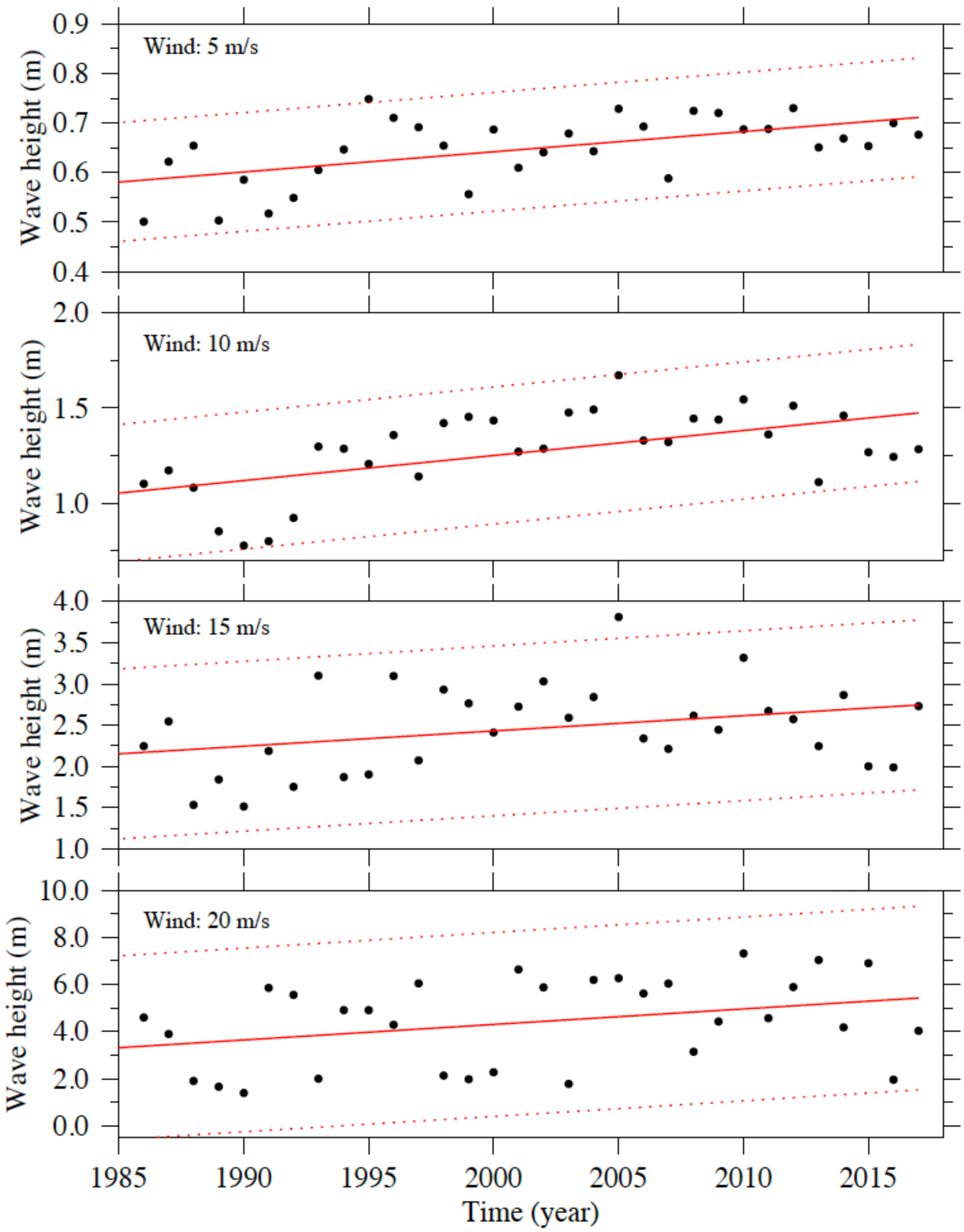

Fig.20: Interannual variability of the significant wave height under given wind speeds of 5, 10, 15, and 20 m/s over 1985-2017, respectively.

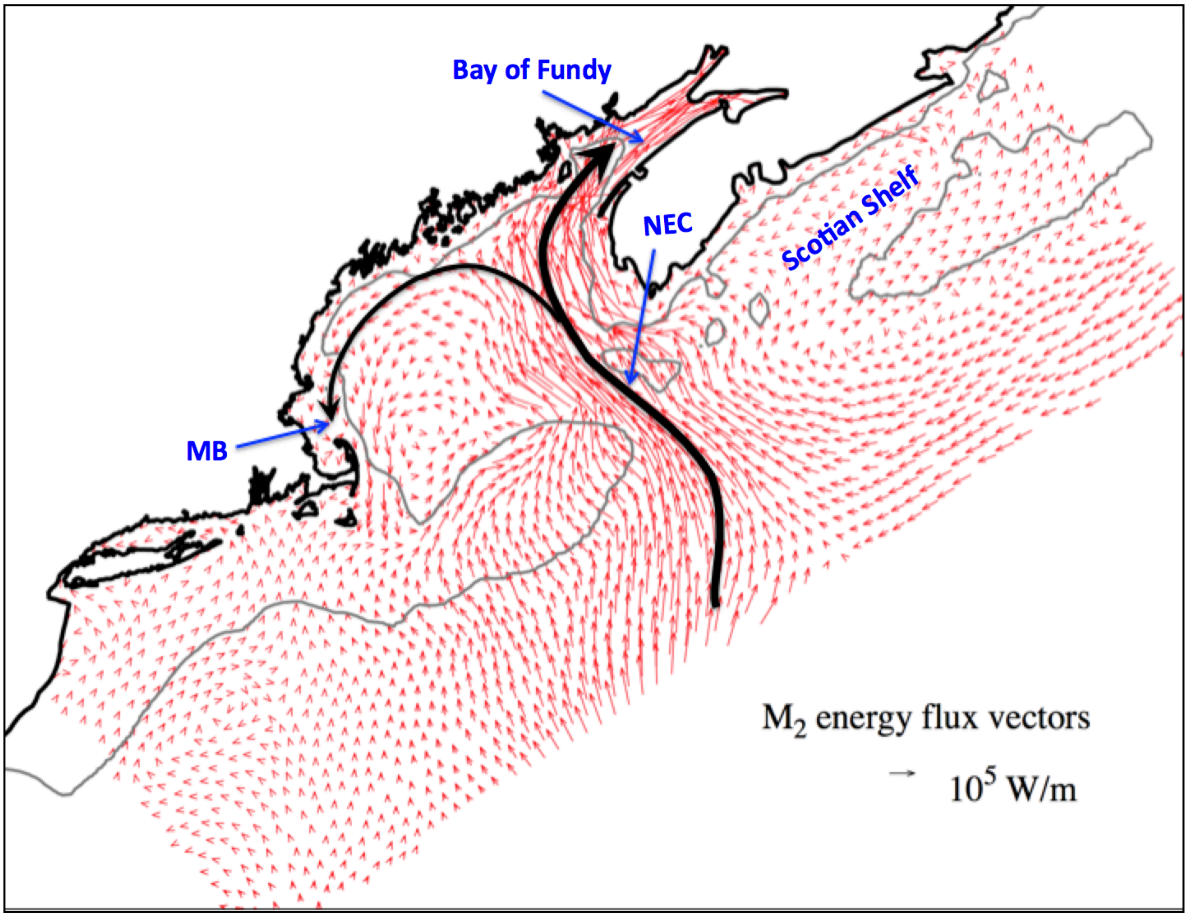

Fig.21: Map of the M2 tidal energy flux vectors in the Gulf of Maine predicted by the NECOFS. MB: Mass Bay, NEC: Northeast Channel.